The Ropelengths of Knots Are Almost Linear in Terms of Their Crossing Numbers

Yuanan Diao, Claus Ernst, Attila Por, and Uta Ziegler

Abstract. For a knot or link $\mathcal{K}$, let $L(\mathcal{K})$ be the ropelength of $\mathcal{K}$ and $Cr(\mathcal{K})$ be the crossing number of $\mathcal{K}$. In this paper, we show that there exists a constant $a > 0$ such that $L(\mathcal{K}) \leq aCr(\mathcal{K}) \ln^5(Cr(\mathcal{K}))$ for any $\mathcal{K}$. This result shows that the upper bound of the ropelength of any knot is almost linear in terms of its minimum crossing number, and is a significant improvement over the best known upper bound established previously, which is of the form $L(\mathcal{K}) \leq O(Cr(\mathcal{K})^{\frac{3}{2}})$. The approach used to establish this result is in fact more general. In fact, we prove that any 4-regular plane graph of n vertices can be embedded into the cubic lattice with an embedding length at most of the order $O(n \ln^5(n))$, while preserving its topology. Since a knot diagram can be treated as a 4-regular plane graph. More specifically, Although the main idea in the proof uses a divide-and-conquer technique, the task is highly non-trivial because the topology of the knot (or of the graph) must be preserved by the embedding.

1. Introduction

In the last 3 decades, knot theory has found many important applications in biology [**16, 20, 21**]. More often than not, in such applications, a knot can no longer be treated as a volumeless simple closed curve in $\mathbb{R}^3$ as in classical knot theory. Instead, it has to be treated as a rope like object that has a volume. For example, it has been reported that various knots occur in circular DNA extracted from bacteriophage heads with high concentration and it has been proposed that these (physical) knots can be used as a probe to investigate how DNA is packed (folded) inside a cell [**1, 2, 3**]. Such applications motivate the study of thick knots, namely knots realized as closed (uniform) ropes of unit thickness. An essential issue here is to relate the length of a rope (with unit thickness) to those knots that can be tied with this rope.

1991 *Mathematics Subject Classification.* Primary 57M25.

Key words and phrases. Knots, links, crossing number, thickness of knots, ropelengths of knots, separators of planar graphs.

Y. Diao is currently supported in part by NSF grant DMS-0712958, C. Ernst and U. Ziegler are currently supported in part by NSF grant DMS-0712997.

To define the ropelength of a knot, one has to define the thickness of the knot first. There are different ways to define the thickness of a knot, see for example [**7, 11, 18**]. In this paper, we use the so called *disk thickness* introduced in [**18**] and described as follows. Let K be a C^2 knot. A number $r > 0$ is said to be *nice* if for any distinct points x, y on K, we have $D(x, r) \cap D(y, r) = \emptyset$, where $D(x, r)$ and $D(y, r)$ are the discs of radius r centered at x and y which are normal to K. The *disk thickness* of K is defined to be $t(K) = \sup\{r : r \text{ is nice}\}$. It is shown in [**7**] that the disk thickness definition can be extended to all $C^{1,1}$ curves. Therefore, we restrict our discussions to such curves in this paper. However, the results obtained in this paper also hold for other thickness definitions with a suitable change in the constant coefficient.

Definition 1.1. For any given knot type $\mathcal{K}$, a *thick realization* K of $\mathcal{K}$ is a knot K of unit thickness which is of knot type $\mathcal{K}$. The *ropelength* $L(\mathcal{K})$ of $\mathcal{K}$ is the infimum of the length of K taken over all thick realizations of $\mathcal{K}$.

The existence of $L(\mathcal{K})$ is shown in [**7**]. The main goal of this paper is to establish an upper bound on $L(\mathcal{K})$ in terms of $Cr(\mathcal{K})$, the minimum crossing number of $\mathcal{K}$.

It is shown in [**4, 5**] that there is a constant $a > 0$ such that for any $\mathcal{K}$, $L(\mathcal{K}) \geq a \cdot (Cr(\mathcal{K}))^{3/4}$. This lower bound is called the *three-fourth power law*. This three-fourth power law is shown to be achievable for some knot families in [**6, 8**]. That is, there exists a family of (infinitely many) knots $\{\mathcal{K}_n\}$ and a constant $a_0 > 0$ such that $Cr(\mathcal{K}_n) \to \infty$ as $n \to \infty$ and $L(\mathcal{K}_n) \leq a_0 \cdot (Cr(\mathcal{K}_n))^{3/4}$. On the other hand, it is known that the three-fourth power law does not hold as the upper bound of ropelengths. In fact, it is shown in [**12**] that there exists a family of infinitely many prime knots $\{K_n\}$ such that $Cr(\mathcal{K}_n) \to \infty$ as $n \to \infty$ and $L(\mathcal{K}_n) = O(Cr(\mathcal{K}_n))$. That is, the general upper bound of $L(\mathcal{K})$ in terms of $Cr(\mathcal{K})$ is at least of the order $O(Cr(\mathcal{K}))$.

In [**15**] it is shown that the upper bound of $L(\mathcal{K})$ is of the order $O(Cr(\mathcal{K}))$ for any Conway algebraic knot. The family of Conway algebraic knots is a very large knot family that includes all 2-bridge knots and Montesinos knots as well as many other knots. The approach used in [**15**] is in fact a simpler version of the divide-and-conquer techniques used in this article. The best known general upper bound of $L(\mathcal{K})$ until now is of order $O((Cr(\mathcal{K}))^{\frac{3}{2}})$, which was obtained in [**13**]. It remains an open question whether $O(Cr(\mathcal{K}))$ is the general ropelength upper bound for any knot $\mathcal{K}$.

In this paper, we prove that the general upper bound of $L(\mathcal{K})$ is almost linear in terms of $Cr(\mathcal{K})$. More specifically, it is established that there exists a positive constant a such that $L(\mathcal{K}) \leq aCr(\mathcal{K}) \ln^5(Cr(\mathcal{K}))$ for any knot $\mathcal{K}$. This is accomplished by showing that a minimum projection of $\mathcal{K}$ can be embedded in the cubic lattice as a planar graph in such a way that the total length of the embedding is of the order at most $O(Cr(\mathcal{K}) \ln^5(Cr(\mathcal{K})))$ and that the original knot can be recovered by some local modifications to this embedding without significantly increasing the total length of this embedding. The construction of the embedding heavily relies on a divide-and-conquer technique that is based on separator theorems for planar

graphs [**19**], but many new concepts and results are also needed in this quest. Overall, this is a rather complicated (at least technically) task that requires attention to many technical details.

The rest of this paper is organized as follows. In Section 2 we introduce the basic concepts of topological plane graphs, cycle cuts and vertex cuts of plane graphs, and some important graph theoretic results concerning these cuts (separator theorems of planar graphs due to Miller [**19**]). In Section 3, we introduce the concept of a class of special plane graphs called BRT-graphs. These are the plane graphs we use as basic building blocks when we subdivide knot diagrams. In Section 4, we apply the separator theorems to show the existence of subdivisions of BRT-graphs. It is a typical divide-and-conquer technique that such subdivisions must be "balanced", that is, each subdivsion produces two smaller BRT-graphs of roughly equal size. We then show that we can apply these concepts recursively subdividing a BRT-graph into smaller and smaller graphs. In Section 5, we introduce the concepts of two special kinds of plane graph embeddings (called "standard 3D-embedding" and "grid-like embedding"). These are not lattice embeddings. The grid-like embedding is almost on the lattice and is used as a basic building block to reconstruct the subdivided graphs. The standard 3D-embedding is used as bench mark for verifying the topology preservation of the reconstructed graphs obtained using the grid-like embedding. Section 6 is devoted to providing detailed descriptions on how to obtain a grid-like embedding of a plane graph either directly, or indirectly from reconnecting two grid-like embeddings of smaller BRT-graphs obtained in the subdivision process. Then in Section 7, we show that a grid-like embedding obtained from reconstruction using our algorithm preserves the topology of the original graph. Section 8 establishes the upper bound on the length of the embedding generated by our embedding algorithm, from which our main theorem result follows trivially. Finally, we end the paper with some remarks and open questions in Section 9.

2. Basic Terminology on Topological Plane Graphs and Cycle Cuts of Weighted Plane Graphs

Throughout this paper, we use the concept of topologically equivalent graphs. In this case, the vertices are points in $\mathbb{R}^3$ and the edges are space curves that can be assumed to be piecewise smooth. If two edges are incident at a vertex or two vertices, then they intersect each other at these vertices, but they do not intersect each other otherwise. A plane ambient isotopy is defined as a homeomorphism $\Psi : \mathbb{R}^2 \times [0,1] \to \mathbb{R}^2$ such that $\Psi(\cdot, t)$ is a homeomorphism from $\mathbb{R}^2$ to $\mathbb{R}^2$ for each fixed t with $\Psi(\cdot, 0) = id$.

A plane graph G refers to a particular drawing of a planar graph on the plane (with the above mentioned conditions, of course). Two plane graphs G_1 and G_2 are said to be *topologically equivalent* if there exists a plane isotopy Ψ such that $\Psi(G_1, 1) = G_2$. It is possible that there are plane graphs G_2 that are isomorphic to G_1 as graphs, but not topologically equivalent to G_1. Since the plane graphs of interest in this paper arise as knot or link projections with the over/under strand

information ignored at the crossings, only topologically equivalent plane graphs are considered. At each vertex v of a plane graph G, a small circle C centered at v is drawn such that each edge of G incident to v intersects C once (unless the edge is a loop edge in such case the edge will intersect C twice). If C is assigned the counterclockwise orientation, then the cyclic order of the intersection points of the edges incident to v with C following this orientation is called the *cyclic edge-order* at v. The following lemma assures that two isomorphic plane graphs are topologically equivalent if the cyclic edge-order is preserved by the graph isomorphism at every vertex. This fact can be easily established by induction on the order of the graph. We leave its proof to our reader as an exercise.

Lemma 2.1. *Let G_1, G_2 be two isomorphic plane graphs with $\phi: G_1 \longrightarrow G_2$ being the isomorphism. If for each vertex v of G_1, the cyclic edge-order of all edges e_1, e_2, ..., e_j (that are incident to v) around v is identical to the cyclic edge-order of $\phi(e_1)$, $\phi(e_2)$, ..., $\phi(e_j)$ around $\phi(v)$, then there exists a plane isotopy $\Psi: \mathbb{R}^2 \times [0,1] \longrightarrow \mathbb{R}^2$ such that $\Psi(G_1, 1) = \phi(G_1) = G_2$. In other words, G_1 and G_2 are topologically equivalent plane graphs.*

Frequently, a plane graph needs to be redrawn differently while keeping its topology. These redrawn graphs occur in rectangular boxes and throughout the paper only rectangles and rectangular boxes whose sides are parallel to the coordinate axes are used. It is understood from now on that whenever a rectangle or a rectangular box is mentioned, it is one with such a property. The following simple lemma is also needed later. It can be proven using induction and the proof is again left to the reader.

Lemma 2.2. *Let R be a rectangle and x_1, x_2, ..., x_n, y_1, y_2, ..., y_n be $2n$ distinct points in R, then there exist n disjoint (piecewise smooth) curves τ_1, τ_2, ..., τ_n such that τ_j starts at x_j and ends at y_j. Furthermore, for any given simply connected region Ω in the interior of R that does not contain any of the points x_1, x_2, ..., x_n, y_1, y_2, ..., y_n, the curves τ_1, τ_2, ..., τ_n can be chosen so that they do not intersect Ω. In fact, many such regions may exist, so long as they do not intersect each other.*

Using this simple fact, it is possible to redraw any plane graph G in any given rectangle such that the vertices of G are moved to a set of pre-determined points in R. This is stated in the following lemma.

Lemma 2.3. *Let G be a plane graph with vertices v_1, v_2, ..., v_n and let R be a rectangle disjoint from G with n distinct points y_1, y_2, ..., y_n chosen. Then there exists a plane isotopy Ψ such that $\Psi(G, 1)$ is contained in R and $\Psi(v_j, 1) = y_j$. Furthermore, for any given simply connected region Ω in the interior of R that does not contain any of the points y_j, Ψ can be chosen so that it keeps Ω fixed.*

Proof. We give a proof for the case that $\Omega = \emptyset$. The case when $\Omega \neq \emptyset$ is left to the reader. A shrinking isotopy Ψ_1 is used such that $\Psi_1(G, 1)$ is contained in a small rectangle R_1 that is small enough to be contained in R. Then R_1 is moved

through a translation to within R such that the vertices x_j of the resulting graph do not overlap with the y_j's. By Lemma 2.2, x_j can be connected to y_j with a curve τ_j such that τ_1, τ_2, ..., τ_n do not intersect each other. Ψ can then be obtained by deforming the plane within R by pushing x_j to y_j along τ_j while keeping the other τ_i fixed, one at a time. □

The following lemma is similar to the above under a different and more restrictive setting. Again this can be proven easily by induction and the proof is left to the reader.

Lemma 2.4. *Let G be a plane graph drawn in a rectangle R. Suppose that R contains n disjoint curves γ_1, γ_2, ... , γ_n which are not closed and are without self intersections. Moreover, these curves do not intersect the vertices of G. Let v_1, v_2, ..., v_k be any k vertices of G ($k \leq |G|$) and x_1, x_2, ..., x_k be any k distinct points in R that are not contained in the curves γ_j, then there exists a plane isotopy that is identity outside a small neighborhood of R as well as on the γ_j and that takes v_j to x_j.*

The following is a 3D variation of Lemma 2.3 which is needed later.

Lemma 2.5. *Let G be a plane graph with vertices v_1, v_2, ..., v_n contained in a rectangle $R \times \{0\}$ in the plane $z = 0$. Let y_1, y_2, ..., y_n be n distinct points in the rectangle $R \times \{t\}$ in the plane $z = t$ for some number $t > 0$. Assume that y_j is connected to v_j by a curve ν_j that is strictly increasing in the z-direction such that the curves ν_j are disjoint, then there exists a 3D isotopy Ψ such that Ψ is level preserving in the z-direction, the identity in the space $z \geq t$ and outside a small neighborhood of $R \times [0, t]$, and $\Psi(\nu_j, 1)$ is a vertical line segment ending in y_j for each j.*

Proof. This is obvious if there is only one curve ν_1. Assume that this is true for $n = k \geq 1$. Then for $n = k + 1$, apply such a level preserving isotopy Ψ_1 to the first k curves. $\Psi_1(\nu_{k+1}, 1)$ is still a strictly increasing simple curve from $\Psi_1(v_{k+1}, 1)$ to y_{k+1}. Modify $\Psi_1(\nu_{k+1}, 1)$ in a level preserving fashion so that its projection to the plane $z = 0$ is a simple curve without self intersection. Now a plane isotopy can be constructed by a push back along this curve from $\Psi_1(v_{k+1}, 1)$ to the projection y'_{k+1} of y_{k+1} to the plane $z = 0$. This does not affect the projections y'_j of the points y_i into the plane $z = 0$ for $j \leq k$. This plane isotopy can be used to define the level preserving isotopy that works for $n = k + 1$ curves. Although there are still some technical details in the argument, it is intuitively obvious at this point and the details are left to the interested reader. □

Remark 2.6. If we relax the condition that the simple curves ν_j's are strictly increasing in the z direction to that they are non-decreasing in the z direction, then one can show that the result of Lemma 2.5 holds without the requirement that the isotopy is level preserving. It is important to note that in this case $\Psi(\cdot, 0)$ is still the identity and $\Psi(G, 1)$ is topologically equivalent to G.

A 3-dimensional ambient isotopy can be similarly defined on $\mathbb{R}^3 \times [0,1]$. However we have to be much more careful about the cyclic edge order at the vertices. For a plane graph the cyclic order of the edges at a vertex is well defined however for a graph in 3 dimensional space it is not. We will fix this problem by requiring that for a graph in 3 dimensional space each vertex v is contained in a small 2 dimensional disk-neighborhood D_v. All the edges that terminate at v intersect D_v in a short arc that terminates at v. The intersection points of these arcs on D_v now define the cyclic edge order at v. We will require that all 3-dimensional isotopies preserve this structure, that is, a 3-dimensional isotopy can move the small disk D_v around in 3-space, it can even deform it, however throughout the isotopy v remains on D_v and all edges terminating at v keep their short arcs on D_v. In this way the cyclic edge order at v remains invariant under the 3-dimensional isotopy. As we will see in Section 5, we use two types of such neighborhoods called blue triangles and red square. Since all 3D-isotopies used in this paper are ambient isotopies that preserve the neighborhood structure of a vertex, we will call them *3D VNP-isotopies* (where VNP stands for "Vertex Neighborhood Preserving").

Definition 2.7. Let G be a plane graph. G is called a *weighted graph* if each vertex, edge, and face of G is assigned a weight (i.e., a non-negative number) and the sum of these weights is 1.

Definition 2.8. Let G be a weighted plane graph. A *cycle cut* of G is a cycle γ in G such that deleting all vertices in γ (and the edges connected to them) divides G into two subgraphs G_1, G_2, on opposite sides of γ, i.e. $G \setminus \gamma = G_1 \cup G_2$. Moreover, if the weights in each G_i sum to no more than α for some real number α, $0 < \alpha < 1$, then the cycle cut is called an α-cycle cut. The *size* of the cycle cut γ is the number of vertices in γ.

The following theorems are proved in [**19**] and play vital roles in the proof of the main theorem of this paper.

Theorem 2.9. [**19**] *Let G be a 2-connected and weighted plane graph such that no face of G has weight more than $2/3$, then there exists a $\frac{2}{3}$-cycle cut of size at most $2\sqrt{2\lfloor d/2 \rfloor n}$, where d is the maximal face size of G.*

If one drops the assumption that G is 2-connected then Theorem 2.9 may not hold since G may be a tree. In this case there is the following theorem.

Theorem 2.10. [**19**] *Let G be a connected and weighted plane graph such that all faces have been assigned weight zero, then either there exists a $\frac{2}{3}$-cycle cut of size $2\sqrt{2\lfloor d/2 \rfloor n}$, or there exists a cut vertex v of G such that each connected component in $G \setminus v$ has a total weight less or equal to $2/3$.*

We refer to the cycle γ that generates a cycle cut as defined by Theorems 2.9 and 2.10 as a *cut-cycle*.

3. Component-Wise Triangulated Plane Graphs: Definitions and Subdivisions

A main tool used to achieve the ropelength upper bound obtained in this paper is the "divide-and-conquer" approach familiar to researchers in graph theory. That is, a knot projection (treated as a 4-regular plane graph) is divided repeatedly using the theorems given in the last section. Several non trivial issues arise in this process. First, the graphs obtained after repeated subdivisions may become highly disconnected. Second, one needs to keep track of the topology of the subdivided piece of the graph so that the pieces resulting from the subdivisions can later be assembled correctly and the original graph can be recovered. This section describes in detail how we handle these problems. The aim is to impose a special structure on the graphs that is preserved after each cut and that this structure allows us to reconstruct the original graph (with the correct topology) from the pieces generated in the divide-and-conquer process.

Definition 3.1. Let G be a connected plane graph without loops. We say that G admits a *proper BR-partition* if the vertices of G can be partitioned into two sets V^B and V^R (called *blue* and *red* vertices, respectively) such that there is no edge between any two blue vertices.

Let G be a plane graph that admits a proper BR-partition with V^B and V^R being the set of blue and red vertices respectively. V^R induces a subgraph $G(V^R)$ of G that is itself a plane graph. A connected component of $G(V^R)$ is called a *red component*. For a red component M, let V_M^R be its vertex set and let V_M^B be the set of blue vertices that are adjacent to some vertices in V_M^R. Let $V_M^* = V_M^R \cup V_M^B$ and let $G(V_M^*)$ be the (plane) subgraph of G induced by V_M^*. $G(V_M^*)$ is called a *BR-component* of G. Notice that under this definition, different BR-components may share common blue vertices, but each edge e of G belongs to exactly one BR-component. A graph is said to be *triangulated* if each face of the graph is either a triangle or a digon.

Definition 3.2. Let G be a connected plane graph that admits a proper BR-partition. G is called a *BRT-graph* if each BR-component $G(V_M^*)$ of G is triangulated. A triangulated BR-component $G(V_M^*)$ is called a *BRT-component*.

Lemma 3.3. *Let G be a BRT-graph, then (i) the boundary of any face of G contains at most one blue vertex and (ii) any cut vertex of G is a blue vertex.*

Notice that condition (ii) above is equivalent to the following statement: for any red component M, the BRT-component $G(V_M^*)$ is 2-connected.

Proof. Suppose that the boundary ∂F of a face F in G contains two different blue vertices v and w. Let P be a path in ∂F that connects v and w which contains at least three vertices, since P cannot be a single blue-blue edge. We assume that v and w and P were chosen so that there are only red vertices on P besides v and w. v and w must belong to $G(V_M^*)$ where M is the red component containing the red vertices on P. It is easy to see that even if P contains only a single red vertex, ∂F

must contain at least 4 edges since v and w cannot be connected by a single edge. This implies that $G(V_M^*)$ is not triangulated, which contradicts the given condition that G is a BRT-graph. This proves (i).

Let v be a cut vertex of G. Then there exists a face F of G such that v appears on ∂F at least twice, i.e., ∂F can be described by a walk $w = P_1P_2$ where P_1 and P_2 are closed walks in G starting and ending at v. P_1 cannot contain only one edge since that would force a loop edge. Thus P_1 contains at least two edges. Similarly, P_2 also contains at least two edges. Thus there exist vertices w_1 and w_2 on P_1 and P_2, respectively, that are adjacent to v. Note that w_1w_2 cannot be an edge in G since v is a cut-vertex. Let us assume that v is a red vertex, and let M be the red component that contains v. Then w_1 and w_2 must also be contained in $G(V_M^*)$ and must be on the same face of $G(V_M^*)$. However this contradicts the assumption that $G(V_M^*)$ is triangulated. Thus v must be blue. This proves (ii). □

For a BRT-graph G, let us define a graph T_G that is associated with G in the following way. Each blue vertex of G corresponds to a vertex in T_G (which is still called a blue vertex) and each red component of $G(V^R)$ corresponds to a vertex in T_G (which is called a red vertex). Vertices of the same color in T_G are never adjacent and a blue vertex x and a red vertex y in T_G are connected by a single edge if and only if the blue vertex v in G corresponding to x is contained in $G(V_M^*)$ where M is the red component corresponding to y. The following lemma asserts that the graph T_G so constructed is a tree.

Lemma 3.4. *The graph T_G defined above is a tree. Equivalently, any cycle in G is contained in a single BRT-component.*

Proof. By construction the graph T_G is a simple bipartite graph since two vertices of different colors can be connected by at most one edge and vertices of the same color are never connected. Moreover there can be no digon in T_G by construction. It follows that a cycle C in T_G (if it exists) must contain at least 4 vertices and the colors of the vertices on the cycle must alternate if one travels along C. Assume that there is a cycle C in the graph T_G which contains a path y_1, x_1, y_2, x_2, y_3 where the x_i are red and the y_i are blue. Let M be the red component of $G(V_M^*)$ which corresponds to x_1. Let y_1 and y_2 be the two blue vertices in C that are adjacent to x_1. Let v_1 and v_2 be the two blue vertices in G that correspond to y_1 and y_2, respectively. The fact that y_1 and y_2 are connected to x_1 in T_G implies that v_1 and v_2 are adjacent to some vertices in M.

The red component M_1 of $G(V^R)$ that corresponds to x_1 divides the plane into one outer face F and several (possibly zero) inner faces. In the interior of each face of M_1 there are blue vertices of $G(V_M^*)$ (if any) or vertices of the other BRT-components besides M_1 (if any). If v_1 and v_2 are both contained in the interior of F, then there exists a path from v_1 to v_2 of the form $v_1r_1...r_kv_2$ where $k \geq 1$ and the path $r_1...r_k$ is contained in ∂F. Since the face in $G(V_{M_1}^*)$ containing this path cannot be triangulated without using blue-blue edges, this is not possible. Thus v_1 and v_2 cannot be both contained in the interior of F. Similarly, on can show that

v_1 and v_2 cannot be both contained in the interior of the same face for any face of M_1. Therefore, one of them, say v_1 is contained in the interior of an inner face F_1 of M_1 and the other v_2 is either contained in the interior of a face F_2 which is either the outer face F or a different inner face.

Since the cycle C has at least length four, there exists a second red vertex x_2 in C neighboring y_2. Let M_2 be the red component of $G(V^R)$ corresponding to x_2. This means that v_2 is connected by an edge to a red vertex in M_2. Since v_2 is contained in the interior of F_2 and G is a plane graph, this implies that M_2 is entirely contained in the interior of F_2. Similarly, continuing to move along the cycle C in the direction established by moving from y_2 to x_2, leads to the conclusion that all blue vertices and red components (of G) corresponding to the vertices on C are contained in the interior of F_2. This contradicts the fact that v_1 is not contained in the interior of F_2. Thus the cycle C cannot exist.

It is easy to see that any cycle passing through more than one BRT-component gives rise to a cycle in T_G. Thus any cycle in G is contained in a single BRT-component of G. □

Let G be a BRT-graph. Let us consider two different ways of dividing G into subgraphs. First, consider the case that G has a cut-vertex v (recall that v must be a blue vertex by Lemma 3.3). Let G_1, G_2, ..., G_k be the connected components of $G \setminus \{v\}$ with V_i being the set of vertices of G_i.

Pick an arbitrary proper subset I_1 of $I = \{1, 2, ..., k\}$ and let $I_2 = I \setminus I_1$. Let $U_1 = \cup_{i \in I_1} V_i \cup \{v\}$ and $U_2 = \cup_{j \in I_2} V_j \cup \{v\}$. Let J_1 be the induced subgraph of G consisting of the BRT-components whose vertices are contained in U_1 and J_2 be the induced subgraph of G consisting of the BRT-components whose vertices are contained in U_2. Note that J_1 and J_2 inherit the plane graph structure naturally from G. In particular, the cyclic ordering of the edges around the vertex v in each subgraph J_1, J_2 is naturally inherited from the cyclic edges ordering around v in G This describes the first kind of subdivision of G which is formally defined below.

Definition 3.5. Let G be a BRT-graph with a cut-vertex v, then dividing G into two subgraphs J_1 and J_2 as described above is called *subdividing G by a vertex-cut.*

Before describing the second subdivision which depends on a cycle of G, we introduce the concept of a *normal cycle*. Let u, v, and, w be three vertices of G such that $uvwu$ is a triangle (namely a cycle with three edges) in G. T he triangle $uvwu$ is empty if it is the boundary of a face of G. A cycle γ in G is said to be *normal* if it contains at least two vertices and no three consecutive red vertices on γ form an empty triangle in G.

Lemma 3.6. *Let G be a BRT-graph. If G has a cut-cycle, then it has a normal cut-cycle.*

Proof. Assume that P is a cut-cycle in G with length ℓ. Then ℓ is at least 2, since G does not contain any loops. If P contains three consecutive red vertices u, v, w which form an empty triangle, then remove v and replace uvw by uw. Since

this operation can never reduce the number of vertices below 2, it always leads to a normal cut-cycle with length at least 2. □

Now let us describe how to use a normal cut cycle γ to divide G. First, γ is pushed off the red vertices by a small distance, resulting in a simple closed curve γ'. The push off γ' is required to have the following properties: (1) All intersections of γ' with the edges of G must happen transversely (except possibly at their endpoints if they are connected to a blue vertex); (2) If v is a blue vertex on γ then v stays on γ'; (3) If e is an edge on γ that is connected to a blue vertex v on γ, then γ' does not intersect e; (4) If e is an edge on γ that is connected to two red vertices, then γ' may intersect e at most once; (5) For an edge e that is not on γ but is connected to exactly one red vertex on γ, γ' can intersect e at most once; (6) For an edge e that is not on γ but is connected to two red vertices on γ, γ' can intersect e at most twice. (The right of Figure 1 shows a non-trivial example of this.) It is easy to see that such a push off is always possible. In addition, if γ' intersects e twice then no empty digons (an empty digon is a digon whose interior or exterior does not intersect G) should be created. The empty digons can always be avoided by routing γ' around the digon as shown in Figure 1. Note that such digons be nested and γ' may have to be pushed across several digons, see Figure 1 on the right.

A simple closed curve γ' obtained from a cycle γ with these properties is called a *push-off* of γ.

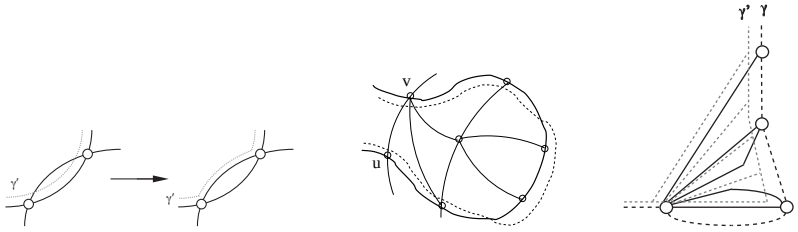

FIGURE 1. γ' intersects an edge twice. Left: Removing empty digons by re-routing γ'. Middle: An edge intersected by γ' (dashed) twice in a non-trivial way. Right: Pushing γ' across several digons.

Let γ be a normal cycle of G and let γ' be a push-off of γ. Let us (temporarily) insert into G a white colored vertex at each intersection point of γ' with the edges of G and a new edge for every arc on γ' connecting two such white vertices or connecting a white vertex and a blue vertex. These white vertices are considered the vertices of γ' and are denoted by $V(\gamma')$. The arcs of $\gamma' \setminus V(\gamma')$ are considered as the edges of γ'.

This graph obtained by adding the edges and vertices of γ' is called G^w. Let $G^w \setminus \gamma'$ denote the plane graph obtained from G^w by deleting all vertices $V(\gamma')$ and the edges connected to these vertices. $G^w \setminus \gamma'$ is separated into two disjoint subgraphs G_I and G_O with G_I inside of γ' and G_O outside of γ'. Let G_I^* be the

subgraph of G^w induced by the vertices $V(G_I) \cup V(\gamma')$. Similarly, let G_O^* be the subgraph of G^w induced by the vertices $V(G_O) \cup V(\gamma')$. Finally, in G_I^* we contract γ' to a single vertex and mark it as a new blue vertex v_1. The resulting plane graph is denoted by G_1'. Similarly, in G_O^* we contract γ' to a single vertex and mark it as a new blue vertex v_2 and call the resulting plane graph G_2'. See Figures 2, 3, and 5 for an illustration of this process.

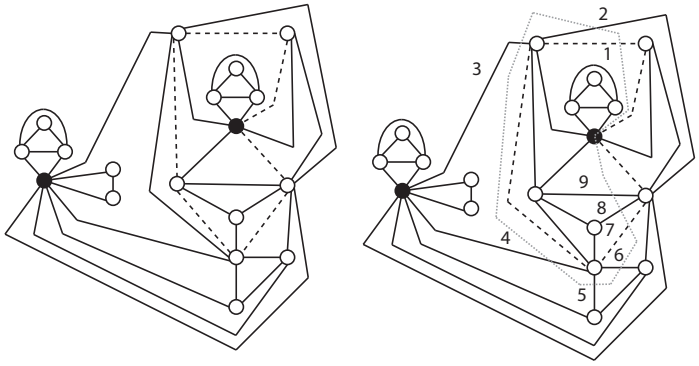

FIGURE 2. Subdividing a plane graph by a edge-cut. Left: a cut cycle γ shown by the dashed edges. Right: the modified normal γ (dashed) and its push-off γ' (dashed and grey). Blue vertices are marked by dark circles and red vertices are marked by while circles. The edges cut by γ' are labeled in cyclic order.

Notice that the cyclic orders of the edges connected to the newly created blue vertices v_1 in G_1' and v_2 in G_2' are inherited from the cyclic order of the intersection points of G with γ'.

Thus G_I^* and G_O^* can be recovered from G_1' and G_2' by expanding v_1 or v_2 back to γ'. G can be recreated by gluing G_I^* and G_O^* along γ' with the original cyclic order of the edges along γ' preserved.

Notice that G_1' and G_2' may not admit a proper BR-partition for two reasons. First, G_1' and G_2' may contain loop edges. Second, the newly created blue vertices v_1 and v_2 (from the contraction of γ') may be adjacent to some other blue vertices in G_1' or G_2' which already exist in G. If this happens in G_i, one of the edges connecting these blue vertices to v_i is simply contracted.

More precisely, assume that w is a blue vertex in G_i' that is connected by several edges $e_1, \ldots, e_k$ to v_i. One of these edges is picked, say e_1 and contracted. This combines w and v_i into one blue vertex - still denoted v_i, and generates $k-1$ loop edges at v_i, see Figure 3. After all blue-blue edges (that are not loop edges) have been eliminated in this way, the resulting (plane) graphs are denoted by G_{1l} and G_{2l}, the l indicating that the graphs may contain loop edges. A loop edge, after it is created, is never cut again, nor does it influence any further subdivisions. Thus there is no reason to keep these loop edges in the plane graphs for the future subdivision process. After deleting the loop edges from G_{1l} or G_{2l}, the resulting

graphs are denoted by G_1 and G_2. Information about γ', the contracted edges, and the deleted loops which are not included in G_1 or G_2 are kept as described later (see Definition 3.9). Only G_1 and G_2 are used in the subsequent subdivisions.

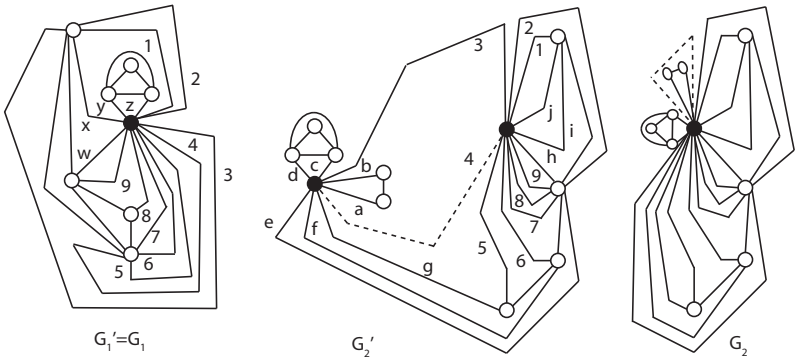

FIGURE 3. The new graphs obtained by subdividing the graph in Figure 2 by γ. Left: G_1 obtained from the subgraph inside γ'. Middle: the graph G_2' obtained from the subgraph outside γ'. Right: G_2, obtained by contracting edge 4 in G_2'. The loop edge created by this contraction (dashed) is deleted from G_2.

Definition 3.7. Let G be a BRT-graph with a normal cycle γ, then dividing G into two plane graphs G_1 and G_2 using a push-off of γ as described above is called *subdividing G by an edge-cut.*

After a BRT-graph G is subdivided into two new plane graphs as described in the above two definitions, are the newly obtained graphs also BRT-graphs? This is not obvious in the case of an edge-cut subdivision since some original BRT-components may have been modified by the subdivision process. The answer to this is affirmative and established in Lemma 3.8 below.

Lemma 3.8. *Let G be a BRT-graph. If G_1 and G_2 are the two graphs obtained after a vertex-cut subdivision or an edge-cut subdivision is applied to G, then G_1 and G_2 are also BRT-graphs.*

PROOF. In the case that G_1 and G_2 are obtained by a vertex-cut subdivision the lemma is obvious. Thus we concentrate on the case of an edge-cut subdivision. By construction the new graphs G_1 and G_2 do not have blue-blue edges. Furthermore, if G is connected, then G_1 and G_2 are also connected. Let γ be the cycle used in this edge-cut subdivision. By Lemma 3.4, γ is contained in a single BRT-component $G(V_M^*)$ for some red component M in G. Obviously, all other BRT-components of G remain unchanged in the subdivision process. These BRT-components remain as triangulated BRT-components in either G_1 or G_2.

Let N be a red component of G_1 that contains some vertices of M. To show that $G(V_N^*)$ is triangulated, it is first shown that all faces in G_1' or G_2' created in

the process of contracting γ' are either triangles or digons. Note that G_1' or G_2' may contain loop edges and those are addressed later. To show that after contracting γ' the resulting graph is still triangulated, the contraction of the edges on γ' is considered one edge at a time.

Let F be a face of $G(V_M^*)$ and let ∂F be its boundary. If the interior of F does not intersect γ', then F is not affected by the contraction process of γ' and it remains a triangle or a digon after the subdivision. If the interior of F and γ' intersect each other, then ∂F must contain at least one vertex on γ. Let e be an edge of γ' that intersects F and assume that e splits F into two faces F_1 and F_2 in G_I^* and G_O^*, respectively. e can intersect ∂F in two white vertices (i.e. in two different edges) or e can intersect ∂F in one white and one blue vertex (i.e. in one edge and the blue vertex of F). It is easy to see that regardless of whether F is a digon or a triangle and regardless of the particular location of these intersections the contraction process changes F_1 and F_2 into loops, digons, or triangles, see Figure 4.

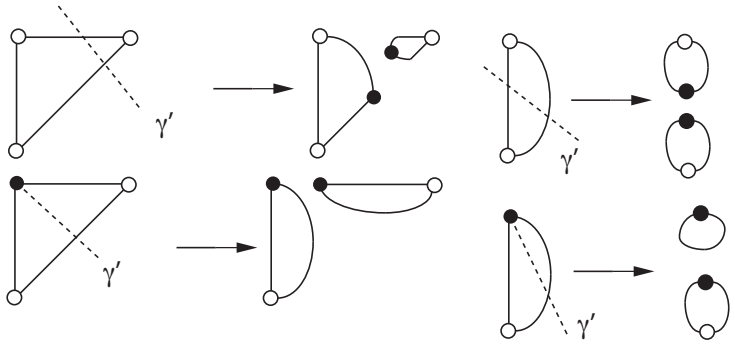

FIGURE 4. The possible cases of how an edge e on γ' can intersect the interior of a triangle or a digon. The three cases for a triangle are on the left, the two cases for a digon are on the right. The resulting faces after γ' (marked by the dashed line) is contracted to the new blue vertex are on the right side of the arrows.

At this point we have established that after the contraction of γ' all faces that are changed by the subdivision remain triangulated in G_1' and G_2'. To obtain G_{1l} and G_{2l}, it is necessary to contract some of the blue-blue edges that may have been created when the new blue vertices were introduced. However, the contraction of an edge in a graph does not increase the size of any face, and thus the triangulation property of all affected faces is preserved. The final step to obtain G_1 and G_2 from G_{1l} and G_{2l} is to delete all loop edges that may have been created in the contraction process of γ' and some of the blue-blue edges. Let e be a loop edge created by this contraction connected to a blue vertex v. Let F_1 and F_2 be the two faces on the different sides of the loop edge e. If both ∂F_1 and ∂F_2 contain vertices different from v then these vertices are red and belong to two different BRT-components (after

the cut). Therefore the face $\partial F_1 \cup \partial F_2$ created by deleting e does not have to be triangulated and e can be deleted. If one, say ∂F_1 contains no other vertices (that is ∂F_1 is consists of one or two edges from v to v) then the deletion of e causes the number of edges in ∂F_2 to remain the same or to decrease by one and thus cannot violate the triangulation property of F_2. Therefore all BRT-components in G_1 and G_2 remain triangulated. □

After a BRT-graph G is subdivided into BRT-graphs G_1 and G_2, it may no longer be possible to reconstruct G from G_1 and G_2 unless information about the subdivision step is kept. For each blue vertex v in G which is not involved in the subdivision process, the order of its edges in G is the order of the edges of the corresponding blue vertex in G_1 or G_2 and no additional information must be kept. The information about the blue vertices involved in the subdivision process is captured in a small neighborhood N. N includes information about the edges involved in the subdivision and their relative order. In addition, for an edge-cut, the neighborhood contains information about the edges contracted (if any) and the loop edges (if any) temporarily created during the subdivision. All loop edges are deleted in the final step of the process that changes G_{il} to G_i.

Notice that all the edges in G are labeled at the beginning and these labels do not change in the subdivision process. Thus the edges in G_1, G_2, and N share the same label if and only if they are part of the same edge in G, therefore the labeled graphs G_1 and G_2 together with N contain all the information needed to reconstruct G (since Lemma 2.1 can then be applied to the reconstructed graph).

The detailed information stored in N is different for a circular edge-cut and for a vertex cut.

(i) For a circular edge-cut, N is an annulus which contains a small neighborhood of $\gamma' \cup E_\gamma$, where E_γ is the set of edges of G^w that are incident to both a white and a blue vertex and that are contracted in the steps of the subdivision process which changes G'_i to G'_{il}, see Figure 5 for an example.

The outside and inside boundaries of N are used to keep track of the cyclic order of the edges of G_1 and G_2 (as well as the deleted loop edges) around their corresponding blue vertices created by the edge-cut. For reasons discussed in Section 5 and in Subsection 5.2 we impose a *linear order* on the edges around a blue v_i^b at the time when it is created in the subdivision process. This is accomplished by identifying a path β in N that connects the inside and outside boundary of N without intersecting any of the edges of G. Cutting N along β results in the linear order of the edges for v_1^b and v_2^b inherited from the counterclockwise orientation on each of the boundary components of N, see Figure 5. From now on, it is understood that the linear order at a blue vertex is so defined if the vertex is created by a circular edge-cut subdivision of a BRT-graph.

A loop may be created and becomes part of G_{il} in two situations. First, if an edge e not on γ is cut twice by γ', (see the right diagram in Figure 1 for an

example) a loop is created in the G_{il} which does not contain the vertices incident to e. In this case the same edge label appears twice on each boundary component of N.

Second, if k red-blue edges $e_1, \ldots, e_k$ with $k > 1$ which are incident to a blue vertex u are cut by γ' (see Figures 2 and 3 for an example), then u is contracted into the v_i^b associated with the G_i' which contains u and $k-1$ loops are created. The loops are in the G_{il} associated with that v_i^b. Here the same edge label appears three times in ∂N for each of these loops: twice on the boundary of the component which contains the loop edge before its deletion and once on the other. Loops are not included in G_i. However, to enable a correct reconstruction of G the information about how the loop connections interleave with other edges cut by γ' is kept by the edge labels on ∂N.

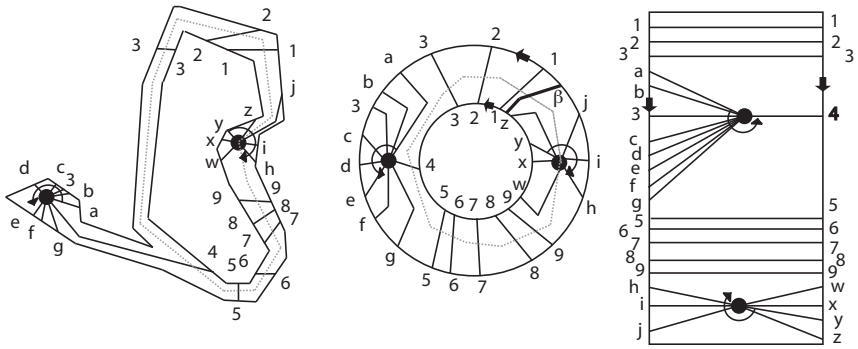

FIGURE 5. Left: the neighborhood N of the edge-cut subdivision of Figures 2 and 3 as it arises in G; Center: N deformed into an annulus together with the path γ', the orientations on ∂N and the path β used to establish the linear order; Right: N (cut open along β) deformed into a rectangle.

(ii) For a vertex-cut subdivision, N is a disk which contains a small neighborhood of v, the cut-vertex used for the subdivision. Once a single point β that does not belong to any edge on the boundary of N is chosen, the linear order of the edges around the new blue vertices v_1^b and v_2^b is inherited from the cyclic order of v.

From now on, it is understood that the linear order is so defined at a blue vertex created by a vertex-cut subdivision of a BRT-graph, see Figure 6. Note that we can indicate the linear order of the edges at a blue vertex v in N by a small circular arrow o_v around a blue vertex. The edge on which the tail of o_v is placed indicates the first edge of the linear order and the arrow head points into the direction of that linear order. Even though we could think of a BRT-graph G as a graph where every blue vertex has an arrow indicating a linear order we are only interested in assigning a linear order (with an arrow) resulting from subdivsions. When we apply an embedding algorithm to a BRT-graphs later in this paper, every

blue vertex originated from a subdivision process and has an assigned linear order. The linear order of the blue vertices in a neighborhood N is included in N. For an example see the two small arrows around two blue vertices in Figure 5. Note that we did not include the small arrows at the blue vertices in Figures 2 and 3, since the linear orders were not relevant to our discussions at that time.

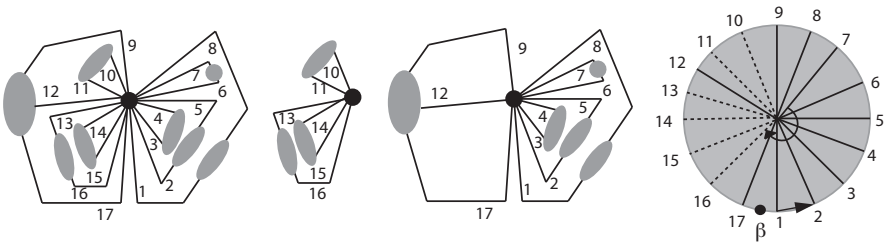

FIGURE 6. Left: The graph G with a vertex-cut at a blue vertex v. The gray shaded ellipses are the different BRT-components that contain the vertex v. These BRT-components can be of any size; Middle: The graphs G_1 and G_2 after the vertex-cut subdivision; Right: The neighborhood N of the blue vertex v containing the gluing instruction, the edges of G_1 are dashed. The arrow on ∂N shows the orientation and the point β is used to define the linear order of the edges.

Definition 3.9. The small neighborhood N addressed above, together with the labels of the edges of G_1, G_2, is called *the gluing instruction* of the corresponding subdivision of G. The orientation of a component of ∂N is called the *orientation vector* of the boundary component.

The information provided by G_1, G_2, and the gluing instruction suffices to reconstruct the graph G uniquely (up to a plane isotopy) by observing that the position of the loop edges (up to a plane isotopy) in G'_{il} can be derived from the given information. For each such loop edge the gluing instruction determines a unique vertex and a unique face that must contain the loop edge and therefore the position of the loop edge is unique (up to a plane isotopy). The reconstruction of G is a reversed process of the subdividing and contracting (used to obtain G_1 and G_2): deleted loop edges are first glued back to G_1 and G_2, the contracted edges (if any) between two blue vertices v_1^b and v_2^b are expanded back, then the blue vertices in G_1 and G_2 resulting from the contraction of γ' are expanded back to a closed curve equivalent to γ' and the edges cut by γ' are glued back together in the last step. This reversed process is made possible since all the information needed is stored in the gluing instruction. We summarize this in the following lemma.

Lemma 3.10. *Let G be a BRT-graph and let G_1 and G_2 be the two BRT-graphs obtained by a vertex-cut subdivision or an edge-cut subdivision of G. Then the planar embeddings G_1 and G_2 induced from G together with the gluing instruction*

that arise from this subdivision allow a reconstruction of a graph that is plane isotopic to the original graph G.

4. Balanced Subdivisions of BRT-graphs and Knot Diagrams

In the last section, it was shown that subdividing a BRT-graph G by a vertex-cut or by an edge-cut (based on a normal cut-cycle) results in two BRT-graphs G_1 and G_2. The main task of this section is to show that it is possible to subdivide a BRT-graph G such that the sizes of G_1 and G_2 are balanced. Recall from the definition of the subdivision that a red vertex of G remains a red vertex in one of G_1 and G_2 (but not both) and no new red vertices are created in the process. That is, if G_1 and G_2 are the graphs obtained from G by subdivision with V_1^R and V_2^R being the sets of red vertices respectively, then V^R is the disjoint union of V_1^R and V_2^R. For a BRT-graph G, let us define its *standard weight* $W_s(G)$ as the number of its red vertices, i.e., $W_s(G) = |V^R|$. If G is subdivided into G_1 and G_2 by a vertex-cut or an edge-cut, then $W_s(G) = W_s(G_1) + W_s(G_2)$. In this section non-standard weight systems are used which are denoted by a lower case w-function.

Definition 4.1. Let G be a BRT-graph and let $c > 0$ be a constant independent of G. A subdivision of G into G_1 and G_2 (by either a vertex-cut or an edge-cut) is *balanced* if $\min\{W_s(G_1), W_s(G_2)\} \geq W_s(G)/6$ and in the case that the subdivision is an edge-cut subdivision, the length of the normal cycle (i.e., the number of red vertices in the cycle) used for the edge-cut is at most $c\sqrt{W_s(G)}$.

In a general BRT-graph, the number of blue vertices may not be bounded above by a function of the number of red vertices as shown in Figure 7. However, if the degrees of the red vertices of a BRT-graph G are bounded above by a constant $g \geq 4$, then the number of blue vertices in G is related to the number of red vertices in G as shown in Lemma 4.2.

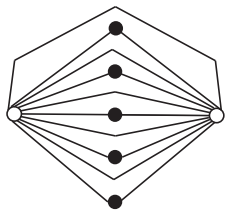

FIGURE 7. A BRT-graph with high blue/red vertex ratio. The red vertices are white and the blue vertices are black.

Lemma 4.2. *Let G be a BRT-graph with $|V(G)| \geq 4$ and g be an upper bound of the degrees of the red vertices, then $|V^B| \leq (g/4)|V^R|$. Consequently, $|V(G)| \leq (1 + g/4)|V^R|$.*

PROOF. It suffices to prove the inequality for a BRT-component $G(V_M^*)$ of G. Deleting all but one edge from each set of multiple edges connecting the same two vertices in $G(V_M^*)$ results in a simple graph H with the same number of blue and

red vertices as that of $G(V_M^*)$. (Here we think of multiple edges as edges that create an empty digon and not just edges that have the same end vertices. For example, the graph in Figure 7 does not have a multiple edge.) Now H has only triangular faces. Let n_r (n_b) be the number of red (blue) vertices in H and let f be the number of faces in H. The boundary of each triangular face contains at least 2 red vertices and any red vertex can be on the boundaries of at most g different faces. Thus n_r is bounded below by $n_r \geq 2f/g$. On the other hand, each blue vertex is on the boundaries of at least two faces and the boundary of each face contains at most one blue vertex (Lemma 3.3). So $n_b \leq f/2 \leq gn_r/4$. □

Lemma 4.3. *Let $g \geq 4$ be a given constant. There exists a constant $W_0 > 3$ such that for any BRT-graph G with $W_s(G) > W_0$ and the maximum degree of the red vertices in G being $\leq g$, there exists a balanced subdivision of G.*

Proof. First consider the case that G contains a BRT-component $G(V_M^*)$ such that $W_s(G(V_M^*)) \geq W_s(G)/2$. (Note that it is possible that $G = G(V_M^*)$.) A non-standard weight system w is assigned to $G(V_M^*)$ as follows. Let $m = |V^R|$ be the number of red vertices in G. Each red vertex in $G(V_M^*)$ is assigned weight $1/m$. All blue vertices in $G(V_M^*)$ are assigned weight zero. Each face f of $G(V_M^*)$ is assigned a weight $w(f) = r_f/m$, where r_f is the number of red vertices of $G \setminus G(V_M^*)$ that are contained in f.

The total weight is equal to 1 since every red vertex of G is either in M or is contained in a face of $G(V_M^*)$. Since $W_s(M) = W_s(G(V_M^*)) \geq W_s(G)/2$, no face of $G(V_M^*)$ has weight larger than $1/2$. Under this non-standard weight assignment, Theorem 2.9 implies that there exists a $\frac{2}{3}$-cycle cut that divides $G(V_M^*)$ (hence G) into two subgraphs. Moreover the length of the cycle γ used is at most $2\sqrt{2n}$ where $n = |V(G(V_M^*))| \leq (1 + g/4)m$ by Lemma 4.2. If γ is not normal, then it can be modified into a normal cut-cycle in $G(V_M^*)$ by Lemma 3.6. The normal cut-cycle γ_1 so obtained is shorter than γ, and each of the two subgraphs separated by it has at most $(2/3)m + 2\sqrt{2n}$ red vertices. Now choose $W_0 > 0$ to be a constant large enough so that $(2/3)m + 2\sqrt{2n} \leq (2/3)m + 2\sqrt{2(1 + g/4)m} < (5/6)m$ holds for every $m > W_0$.

Next consider the case that every BRT-component $G(V_M^*)$ has a standard weight $W_s(G(V_M^*)) < W_s(G)/2 = m/2$ (where $m = |V^R|$). Let T_G be the tree defined in Section 3 (before Lemma 3.4). A red vertex v_M of T_G that corresponds to a red component M is assigned the weight $w(v_M) = W_s(M)/m$. All blue vertices of T_G are assigned weight zero. Notice that under this weight assignment, the total weight is 1. Thus by Theorem 2.10 there exists a cut-vertex v in T_G such that each connected component in $T_G \setminus \{v\}$ has a total weight less than or equal to $2/3$. If v is a blue vertex in T_G, then the blue vertex u in G corresponding to v is a cut vertex and can apparently be used to obtain a balanced vertex-cut subdivision of G. (A vertex-cut using the cut vertex u obtained in this manner in facts leads to connected components each of which has a weight of $2m/3$ or less.) On the other hand, if v is a red vertex then it corresponds to a red component M of $G(V^R)$.

Assign $G(V_M^*)$ the non-standard weight system w_1 as before: each red vertex in M is assigned the weight $1/m$, each blue vertex in $G(V_M^*)$ is assigned weight zero, and each face f of $G(V_M^*)$ is assigned the weight $w(f) = r_f/m$, where r_f is the number of red vertices of $G \setminus G(V_M^*)$ that are contained in f. Again the total weight is 1 since every red vertex of G is either in M or is contained in a face of $G(V_M^*)$. No face f in $G(V_M^*)$ has a weight $w(f) > 2/3$ since otherwise deleting the red vertex v in T_G corresponding to M results in a connected component in T_G with weight $> 2/3$, contradicting the given property of v. Thus by Theorem 2.9 there exists a cycle γ in $G(V_M^*)$ that yields a $\frac{2}{3}$-cycle cut of G. Again modify γ as before to obtain a normal cycle γ_2 and use γ_2 to obtain an edge-cut subdivision of G. The only difference is that this time γ_2 causes a smaller bound on W_0 since the weight of $G(V_M^*)$ is less than $m/2$, so the total weight of each of the two graphs obtained by the edge-cut using γ_2 is bounded above by $(2/3)m + 2\sqrt{2n} < (5/6)m$ where $n \leq (1 + g/4)m/2$ is the number of vertices in $G(V_M^*)$. □

The definition of a (balanced) vertex-cut may allow many different choices for G_1 and G_2 by choosing different unions of BRT-components. In order to allow a successful reconstruction, constraints are imposed on the selection of the BRT-components for G_i for a balanced vertex-cut. Lemma 4.4 specifies these constraints and asserts that they can always be met.

Assume that G is a BRT-graph and v is a blue vertex in G that can be used for a balanced vertex-cut. Let α be an arc that starts and ends at v and is otherwise disjoint from G. α separates G into two subgraphs G_1 and G_2 both containing v and that are unions of complete BRT-components. We call G_1 (and G_2) a *disk-component* of G. It is possible that one of the two graphs contains only the vertex v. However, if both G_1 and G_2 contain at least one vertex other than v, then G_1 and G_2 are called *proper disk-components* of G. A disk-component H is *separable* if there exist two proper disk-components H_1 and H_2 such that $H = H_1 \cup H_2$ and H_1 lies in the outer face of H_2. H is called *inseparable* if it is not separable. H' is a *maximal disk-component* of H if H' is a proper disk-component contained in H and if for every disk-component D in H that contains H' either $D = H'$ or $D = H$. See Figure 8.

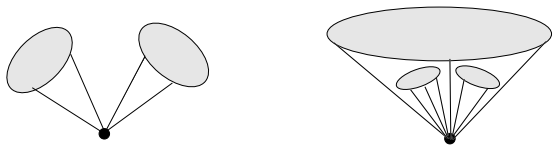

FIGURE 8. Left: A separable disk-component; Right: An inseparable disk component containing two maximal disk-components. A gray area indicates BRT components as in Figure 6.

Lemma 4.4. *Let G be a BRT-graph that admits a balanced vertex cut using the cut-vertex u (in G), where u is a cut vertex obtained as in the proof of Lemma 4.3.*

Let G_1 and G_2 be the two subgraphs obtained by the vertex-cut. Then one of the subgraphs, say G_1, can be chosen as one of the following:

(i) G_1 is a disk-component of G.

(ii) G_1 consists of a union of several maximal disk-components of a single inseparable disk-component of G.

Notice that Figure 6 is an example of case (ii).

PROOF. If there exists a disk-component H of G with $W_s(G)/6 \leq W_s(H) \leq 5W_s(G)/6$ then let G_1 be H (case (i)). Now assume that no disk-component H exists in G such that $W_s(G)/6 \leq W_s(H) \leq 5W_s(G)/6$. Assume there exists a disk-component H of G such that $W_s(H) > 5W_s(G)/6$. Moreover assume that among all disk-components H with $W_s(H) > 5W_s(G)/6$, H is the smallest one.

Claim 1: H must be inseparable. Otherwise, $H = H_1 \cup H_2$ for two disjoint proper disk-components H_1 and H_2. H_1 or H_2 must have weight less than or equal to $5W_s(G)/6$ since H is the smallest disk-component with weight more than $5W_s(G)/6$. But then it must be true that $W_s(G)/6 \leq W_s(H_1) \leq 5W_s(G)/6$ or $W_s(G)/6 \leq W_s(H_2) \leq 5W_s(G)/6$ since $W_s(H_1) + W_s(H_2) = W_s(H) > 5W_s(G)/6$. This is a contradiction since we assumed that there are no disk-components with weight between $W_s(G)/6$ and $5W_s(G)/6$.

Claim 2: H must contain at least one proper disk-component H' with $W_s(H') < W_s(H)$. If this is not the case, deleting u from G results in a connected component of weight more than $5W_s(G)/6$, contradicting the fact that u is a cut-vertex for a balanced vertex cut. Remember that the cut-vertex u obtained in the the proof of Lemma 4.3 leads to connected components with weights $\leq 2/3W_s(G)$.

It follows that H contains maximal proper disk-components. Let $H_1, H_2, \ldots, H_k$ be the maximal proper disk-components of H, then for each i, $W_s(H_i) < W_s(G)/6$ by our assumptions. Let $W_s = \sum_i W_s(H_i)$. We must have $W_s \geq W_s(H)/6$, otherwise the graph $H \setminus (\cup_i H_i)$ has weight $> 5W_s(G)/6 - W_s(G)/6 = 2W_s(G)/3$ and remains connected after u is deleted, contradicting the fact that u is a cut-vertex for a 2/3-balanced vertex cut. Thus G_1 can be chosen to be the union of some or all of the H_i's (case (ii)). The last case we need to consider is that all disk-components H of G satisfy the condition $W_s(H) < W_s(G)/6$. However this is impossible since G is a disk-component of itself. □

In order to apply the divide-and-conquer technique, it is necessary for us to use repeated balanced subdivisions to a BRT-graph G.

Definition 4.5. A BRT-graph G (and the resulting BRT-subgraphs) can be divided recursively using balanced subdivisions. When the standard weight of a BRT-graph obtained in this repeated subdivision process falls below a pre-determined threshold W_0, the subdivision process stops on this BRT-graph and it is called a *terminal BRT-graph*. The subdivision process has to terminate at the point when all the resulting BRT-graphs are terminal BRT-graphs. The balanced subdivisions used to reach this stage are called a *balanced recursive subdivision sequence* of G.

To keep track of the BRT-graphs obtained when a balanced recursive subdivision sequence is applied to a BRT-graph G, the following notations are adopted. $G(0,1) = G$. When the first subdivision is applied, the two resulting BRT-graphs are denoted by $G(1,1)$ and $G(1,2)$, the gluing instruction of the subdivision process is denoted by $N(0,1)$, and the two new blue vertices created are denoted by $v^b(1,1)$ and $v^b(1,2)$. The two BRT-graphs obtained from subdividing $G(1,1)$ are denoted by $G(2,1)$ and $G(2,2)$ and the two BRT-graphs obtained from subdividing $G(1,2)$ are denoted by $G(2,3)$ and $G(2,4)$, and so on. In general, the BRT-graphs obtained from subdividing $G(i,j)$ (if $W_s(G(i,j)) > W_0$) are denoted by $G(i+1,2j-1)$ and $G(i+1,2j)$, the newly created blue vertices are $v^b(i+1,2j-1)$ and $v^b(i+1,2j)$, and the gluing instruction is $N(i,j)$. See Figure 9 for an illustration of this relation. Notice that the lengths of the paths from the root ($G(0,1)$) of the tree to the leaves are not necessarily the same as shown in Figure 9, since some BRT-graphs may terminate earlier than others due to size differences. We say that a BRT-graph H is *induced* from the plane graph G if H is one of the $G(i,j)$s described above. If $G(i_0,j)$ is a terminal BRT-graph where i_0 is largest among all other terminal BRT-graphs induced from $G(0,1)$ (from the same recursive subdivision sequence), then i_0 is called the *depth* of the corresponding recursive subdivision sequence.

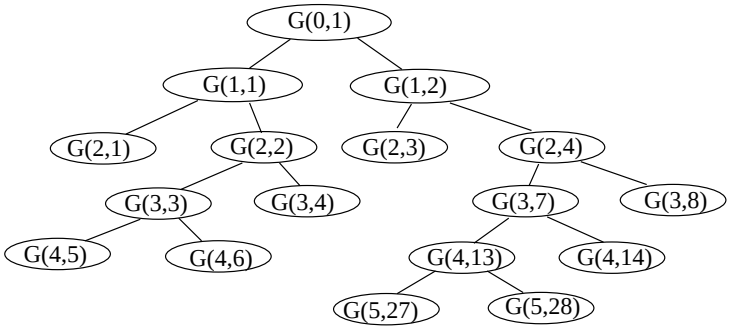

FIGURE 9. The tree structure of BRT-graphs obtained from a balanced recursive subdivision sequence of G.

Lemmas 3.8 and 4.3 lead to the following theorem.

Theorem 4.6. *There exists a balanced recursive subdivision sequence for each BRT-graph G. Furthermore, $W_s(G(i,j)) \leq |V^R(G)|(5/6)^i$ since the subdivisions are balanced. It follows that there exists a constant $c_r > 0$ (c_r depends only on W_0 and the maximal degree g of all the red vertices in G) such that the depth of any balanced recursive subdivision sequence of G is bounded above by $c_r \ln(|V^R(G)|)$.*

Remark 4.7. Let i_0 be the depth of a balanced recursive subdivision sequence of G and $G(i,j)$ be one of the BRT-graphs induced from G by this sequence. If we apply Theorem 4.6 with $G(i,j)$ playing the role of G (as the starting graph in the subdivision sequence), then the depth d of the subdivision sequence leading $G(i,j)$ to its terminal BRT-graphs is at most $i_0 - i$ and we have $d \leq c_r \ln(W_s(G(i,j)))$.

To apply the recursive subdivision to a knot diagram, we start with a minimum knot diagram D of the knot $\mathcal{K}$ so that the number of crossings in D is equal to $n = Cr(\mathcal{K})$. Ignoring the over/under information of D at its crossings, we treat D as a 4-regular plane graph. In general, D is not a BRT-graph since D may contain faces of arbitrarily large size. Thus the previously established results cannot be applied directly to D. To remedy this problem, artificial edges are added to D so that the resulting graph is a BRT-graph. These added edges may simply be removed from the embedding of the modified graph at the end of the process. The following lemma asserts that D can be modified into a BRT-graph in such a way that the maximum degree of its vertices is bounded by a constant.

Lemma 4.8. *Let D be a minimum projection of $\mathcal{K}$. If D is treated as a plane graph so that crossings of D are treated as vertices and strands connecting crossings are treated as edges, then by simply adding some new edges to D, D can be modified into a plane graph G such that G is triangulated and the maximum degree of the vertices of G is bounded above by 12.*

Proof. Each face F of D can be triangulated in a way as shown in Figure 10. In doing so, at most two edges are added to a vertex of F. Since each vertex in D belongs to at most 4 faces this results in at most 8 new edges being added to each vertex. Hence the maximum degree of the resulting graph is bounded above by 12. □

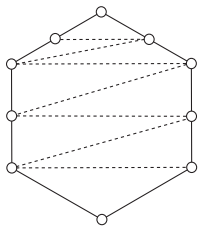

Figure 10. Triangulation of a face of a 4-regular plane graph by adding new edges. The edges added in the triangulation are dashed.

Let G be the triangulated graph obtained from D as described in the proof of Lemma 4.8. At this stage, every vertex in G is considered to be a red vertex. Since G contains no blue vertices and no loop edges, it admits a proper BR-partition. Furthermore, it contains only one red component (namely itself) and this component is triangulated. Thus by definition, G is a BRT-graph (without blue vertices). By Theorem 4.6, there exists a balanced recursive subdivision sequence for G. Since the subdivision operations do not increase the degree of a red vertex, the maximum degree of red vertices in such a graph H is still bounded above by 12, see Lemma 4.8.

5. Standard 3D-embeddings and Grid-like Embeddings of BRT-graphs

In this section we introduce two special kinds of embeddings: the standard 3D-embedding and the grid-like embedding. The purpose of introducing the standard 3D-embeddings of BRT-graphs is to use these embeddings as benchmarks to verify that the topology of a graph is preserved when it is reconstructed from its two induced BRT-graphs. On the other hand, the purpose of introducing the grid-like embeddings is to simplify the reconstruction process: if two induced BRT-graphs are grid-like, then their grid-like structure will allow us to reconnect them in a way to preserve this grid-like structure so this reconnected graph can be used again in the next round of the reconstruction process of G. Furthermore, a grid-like embedding is almost on the lattice and in the last step when $G = G(0,1)$ itself is reconstructed (from its two immediate induced BRT-graphs $G(1,1)$ and $G(1,2)$), it will be easily modified into a lattice embedding.

5.1. Standard 3D-embeddings. In the following we assume that all BRT-graphs $G(i,j)$ involved are induced from a plane graph G and that the maximum degree of red vertices is bounded above by 12. Below we are introducing some terminology that we will use for the graphs $G(i,j)$ and their blue vertices throughout the next sections.

Rectangles. Since $H = G(i,j)$ is a plane graph drawn in the plane $z = 0$, it can be embedded in the interior of a rectangle R in the plane $z = 0$. That is, there exists a plane isotopy $\Psi : \mathbb{R}^2 \times [0,1] \longrightarrow \mathbb{R}^2$ such that $\Psi(x,0) = id$ and $H_1 = \Psi(H,1) \subset (R \setminus \partial R)$. We will assume that all graphs $H = G(i,j)$ are contained in such a rectangle. Keep in mind that our the sides of our rectangles are parallel to either the x-axis or the y-axis.

Blue squares. For each blue vertex v of H create a small square S_v^b in the plane $z = 0$ with side length 3ℓ for some fixed small positive number $\ell > 0$ such that v is at the center of the square and $S_v^b \subset (R \setminus \partial R)$. S_v^b is called a *blue square*. See Figure 11.

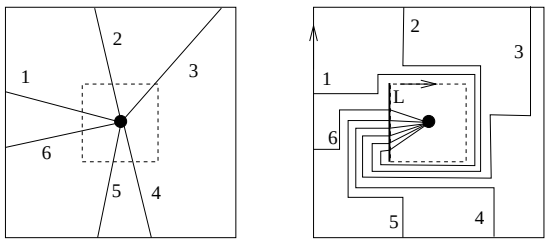

FIGURE 11. Left: A blue square; Right: A blue square with edges inside it re-routed through a side L (marked by the thickened line segment). The edge with label 1 is the first edge in the linear order assigned at the blue vertex.

Without loss of generality we can assume that the boundary of S_v^b intersects each edge leading out of v exactly once transversely. Notice that we can isotope the graph locally so that the edges within S_v^b are single line segments as shown on the left of Figure 11.

Let R_v be the square with side length ℓ and center v and L be a side of R_v. The purpose of R_v and L is for us to use a local (VNP-)isotopy to re-route the edges connected to v in such a way that they all enter R_v from L. Moreover within S_v^b the edges use only segments parallel to the x- and y-axis. The right side of Figure 11 then shows an example of how to re-route these edges within $S_v^b \setminus R_v$ to achieve the desired result. As the figure shows, this can be done for each edge in S_v^b involved with at most six right angle turns in the xy-plane. Let e_v be the vector (parallel to either the x- or the y-axis) that points perpendicular from L to v and we call e_v an *extension vector*.

Orientation assignment of ∂S_v^b. Without loss of generality we can assume that the boundary of S_v^b intersects each edge leading out of v exactly once transversely. Recall that when a new blue vertex is created by an edge-cut subdivision, we oriented the components of ∂N counterclockwise and used this orientation to define the cyclic order of the edges intersecting ∂N. If a new blue vertex $v = v^b(i,j)$ is in the BRT-graph $G(i,j)$ obtained by using the part of the original graph outside of γ', then one may treat ∂S_v^b as a deformation (contraction) of the outer component of ∂N. In this case we give ∂S_v^b a counterclockwise orientation. On the other hand, if $v = v^b(i,j)$ is in the BRT-graph obtained using the part of the original graph inside of γ', then ∂S_v^b should be treated as a deformation of the inner component of ∂N, where one would have to flip the inner component of ∂N to realize the resulting graph on the plane without edge crossings. Thus in this case we will assign ∂S_v^b a clockwise orientation. Finally, in the case that v is created by a vertex-cut subdivision, ∂S_v^b is always assigned the counterclockwise orientation.

The orientation vector. The order of the intersection points on L is inherited from the order of intersection points on the boundary of S_v^b induced by the orientation of S_v^b. To be more precise, we can choose any edge on the boundary of S_v^b and using any path to connect it to L. After that we can choose a second edge to go on either side of the first edge along L. After that the order of all other intersection points on L is determined. In the example of Figure 11 we chose L to be on the left side of R_v. Once we fix the edge with label 1 anywhere on L then there are only two choices for the other edges to follow: we can obtain edge order $\{1,2,3,4,5,6\}$ ascending along L, or an edge order of $\{2,3,4,5,6,1\}$ ascending along L. We can think of both of these as the same orientation along L with the difference that one starts with the edge labeled 1 and the other with the edge labeled 2. Thus the counterclockwise or clockwise cyclic order of the edges around S_v^b introduces a unique direction on L. We call the vector given by this orientation the *orientation vector* o_v. Furthermore, we will choose the first edge to intersect L so that the linear order so obtained on L matches the linear order at v_b, i.e. the linear order obtained from the counterclockwise orientation on ∂N together with the choice of

the path β in N (edge-cut) or the point β on ∂N (vertex-cut) as given by the gluing instructions.

Notice that we use the same name and symbol for the small circular arrow around blue vertices in a neighborhood N that contains the glueing instructions, see Definition 3.9. We also use the word orientation vector of the orientation on ∂N. The reason is that these orientation vectors in N or on ∂N directly induce the orientation vector along the segments L. The vectors are equivalent (they tell us the linear order) and this justifies the identical names.

It follows that the extension vector e_v can be obtained from the orientation vector o_v by a 90 degree clockwise or counterclockwise rotation. In the example of Figure 11 we need to rotate the the orientation vector o_v 90 degree clockwise to obtain the extension vector e_v. This tells us that in this case v arose in an edge-cut and belongs to G_1 (the graph obtained from the inside of γ'). If we need to rotate the orientation vector o_v 90 degree counter clockwise to obtain the extension vector e_v then the vertex v arose in a vertex-cut or v arose in an edge-cut and belongs to G_2 (the graph obtained from the outside of γ').

Finally, if in the formation of a blue vertex v an edge between a newly temporarily created blue vertex and an older existing blue vertex is contracted, then the above orientation determination still applies: The linear order of the intersection points on ∂N does include the edges from the existing blue vertex and these existing orders do not change when the blue vertices are merged.

Blue bands and blue triangles. Let L_v be the cross-section of R_v that contains the blue vertex v and is parallel to L and let L'_v be the line segment obtained by moving L_v up to the plane $z = t_1 > 0$ for some positive t_1. Let $\delta > 0$ be a small positive real number and let P be the point directly over v in the plane $z = t$ where $t = t_1 + \delta$. The rectangle formed defined by L_v and L'_v is called a *blue band* and is denoted by B_v. The (vertical) triangle formed by L'_v and P is called a *blue triangle* and is denoted by T_v. We will now redraw the graph locally within the boundary of $R_v \times \mathbb{R}^+$ as shown in Figure 12. Under this redrawing, the point P becomes the blue vertex v and each edge from the boundary of S_v^b to v_b is replaced a path consisting at most 9 straight line segments: at most 7 in the xy-plane, one vertical (from L_v to B_v) and one slant (from B_v to P). This obviously does not change the topology of the graph, it simply creates a 3-D structure of the graph for us to work with. We place the extension vector e_v at the point P for future references. See Figure 12 for an illustration of this. Note that half of R_{v_b} with L_{v_b} as a side but opposite to L is not occupied by any edge under this construction.

Assume that the above process is applied to every blue vertex in the graph, then we arrive at a new graph H_s that is bounded in the rectangular box $B = R \times [0, t]$. Finally, we require that the projections of the blue squares to the x-axis and to the y-axis do not overlap each other. This can be done since we can pre-determine the positions of the blue vertices in R by Lemma 2.4 and we can choose the side length of these squares arbitrarily small.

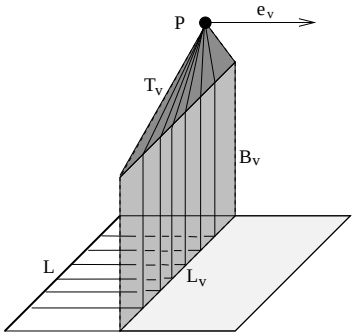

FIGURE 12. An illustration of blue band and blue triangle: the construction only occurs within a rectangular box of height t with R_v as its base. The unused area in R_v is lightly shaded.

Definition 5.1. The embedding H_s obtained in the above process from the BRT-graph H in the rectangular box B is called a *standard 3D-embedding* .

Notice that a standard 3D-embedding H_s of H is isotopic to the BRT-graph H by a VNP-isotopy that is the identity outside the space $R \times [-\epsilon, t+\epsilon]$ for an arbitrarily small positive constant ϵ. Let us first describe the part of the isotopy that involves the space $z > 0$. Here at each blue vertex v we retract the blue band B_v until the base of the blue triangle reaches the plane $z = 0$. After that we fold the blue triangle rigidly into the half of R_{v_b} that is not occupied by any edge. This give us an embedding that is entirely contained in the plane $z = 0$. The rest of the VNP-isotopy involves only moves within the plane (which is a plane isotopy that is automatically VNP). In other words, the VNP-isotopy described here is just a trivial extension of a plane isotopy.

From Lemma 2.3 we know that we may pick the locations of the deformed blue vertices on the top of the box $R \times [0, t]$ with almost total freedom. Therefore, we like to have standard 3D-embeddings of H with the property defined in the following definition.

Definition 5.2. Let H be a BRT-graph induced from G with blue vertices $\{v_1, \ldots, v_k\}$. Let R be any given rectangle in $z = 0$ whose sides are parallel to either the x- or y-axis. Let Q_1, Q_2, ..., Q_k be any k distinct points in the interior of R and let P_1, P_2, ..., P_k be the corresponding points on the plane $z = t$ directly above the points Q_1, Q_2, ..., Q_k. If there exists a standard drawing H_s of H in $R \times [0, t]$ such that P_j is the blue vertex in H_s corresponding to v_j for $j = 1, 2, ..., k$, then H_s is called pre-determined standard 3D-embedding of H (with P_1, P_2, ..., P_k being the pre-determined blue vertices).

The following lemma asserts that it is indeed possible to create pre-determined standard 3D-embeddings of H.

Lemma 5.3. *Let H be a BRT-graph induced from G with k blue vertices and let R be any given rectangle in $z = 0$ whose sides are parallel to either the x- or y-axis. Let Q_1, Q_2, ..., Q_k be any k distinct points in the interior of R and let P_1, P_2, ..., P_k be the corresponding points on the plane $z = t$ directly above the points Q_1, Q_2, ..., Q_k. Then there exists a pre-determined standard 3D-embeddings of H with P_1, P_2, ..., P_k being the pre-determined blue vertices.*

PROOF. Let H be a BRT-graph induced from G with blue vertices $\{v_1, \ldots, v_k\}$. Let R be any given rectangle in $z = 0$ whose sides are parallel to the x- and y-axis. Let Q_1, Q_2, ..., Q_k be any k distinct points in the interior of R. Then by Lemma 2.3 there exists a plane isotopy Ψ such that $\Psi(G, 1)$ is contained in R and $\Psi(v_j, 1) = Q_j$. We can then obtain the desired pre-determined standard 3D-embedding of $\Psi(G, 1)$ with the P_js being the blue vertices of the new graph by the previously outlined construction. □

5.2. Grid-like Embeddings. For the purpose of embedding the graph G into the cubic lattice, the structure offered by a standard 3D-embedding is not enough. We need to use a structure that is almost like a lattice embedding for the graphs obtained in the subdivision process. A graph embedding with such a structure will be called a *grid-like* embedding. The detailed description of this embedding is given in this section.

Assume that $H = G(i, j)$ for some valid i, j from the recursive subdivision process and that the degree of any red vertex in G is at most 12.

Definition 5.4. We call an embedding H_{gr} of a BRT-graph H a grid-like embedding if it satisfies the following conditions:

(i) All red vertices of H_{gr} are lattice points in the plane $z = 0$. Moreover, each red vertex v is contained in the interior of a lattice rectangle S_v^R of dimensions $w \times l$ where $w, l \geq 3$ (called a *red square*) that does not contain any other vertices of H_{gr}. The edges of H_{gr} connected to v must pass through (different) lattice points on the boundary of S_v^R. Figure 13 shows this for a vertex of degree 12 in the smallest possible lattice rectangle (a 3×3 square).

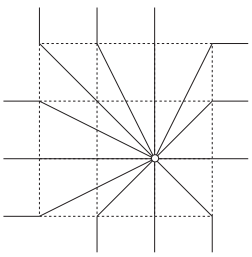

FIGURE 13. A red vertex of degree at most 12 can be realized in a (red) 3×3 lattice square.

(ii) H_{gr} is contained in a rectangular box $B = R \times [0, t]$ for some integer $t > 0$. All blue vertices of H_{gr} are on the top of the box, i.e., in $R \times \{t\}$. Similar to the

standard 3D-embedding, each blue vertex is the top vertex of a blue triangle that is on top of a blue band originated from a blue square. The difference here is that the blue square (from where the blue band originates) may be in a horizontal plane $z = h$ for some integer $0 < h < t - \delta$ (it can also be in the plane $z = 0$), here $\delta > 0$ is a small positive constant. All the other requirements on the blue bands, triangles, and squares as given in the definition of a standard 3D-embedding must also be satisfied.

(iii) All edges outside the red squares and blue triangles are paths consisting of only line segments parallel to the x-, the y-, or the z-axis. Moreover all horizontal line segments must have integer z-coordinates.

(iv) All red-red edges (edges connecting two red vertices) are on the (cubic) lattice with the (possible) exception of the segments contained in red squares. The red-blue edges do not have to be on the lattice.

(v) H_{gr} is isotopic to a standard 3D-embedding of H by a VNP-isotopy ϕ that is identity outside the box $R \times [-1, t - \delta]$. Furthermore the isotopy restricted to any red square must be a plane isotopy, that is throughout the isotopy a red square remains in the plane $z = 0$. However it does not need to remain a lattice rectangle, the red square simply will play the role of a disk neighborhood of the red vertex.

The requirement that the VNP-isotopy is the identity outside the box $R \times [-1, t - \delta]$ enforces that the edge order of the blue vertices cannot be changed since the blue triangles do not move at all. The requirement on the red squares enforces that the edge order of the red vertices cannot be changed either. The reason for the extension $-1 \leq z < 0$ of the space the isotopy can use will become clear later.

6. Grid-like Embeddings of BRT-graphs Induced from a Knot Projection

There are two approaches to obtain a grid-like embedding of a BRT-graph H. The first is a direct construction from the graph H and the second is a reconstruction using two grid-like embeddings of the two BRT-graphs obtained from H by a vertex-cut or an edge-cut subdivision. For the terminal BRT-graphs obtained from G in the subdivision process, we will have to use the first approach to obtain their grid-like embeddings. Although we can use this first approach to get a grid-like embedding of G itself as well, it will not achieve the desired efficiency in the embedding length. For that we will then need the second approach to assemble these grid-like embeddings of the terminal BRT-graphs into grid-like embeddings and ultimately obtain a grid-like embedding of G (which will then be modified into a lattice embedding of the knot diagram).

6.1. Grid-like embedding via direct construction.

The following lemma assures that the first approach is always possible.

Lemma 6.1. *A grid-like embedding of a BRT-graph H can be directly constructed from H.*

PROOF. Let H_1 be a standard 3D-embedding of H that is guaranteed by Lemma 5.3. We stretch R in the x- and y-direction by inserting additional lattice lines. First we add lattice lines at the locations of the red vertices to put these on lattice. Next we add enough lattice lines to create required minimum size red rectangle.

By induction on the number of edges in H_1, we can prove that all edges, except the parts contained in the red rectangles S_i's can be straightened by a VNP-isotopy so that they consist of only line segments parallel to a coordinate axis. We now stretch R in the x- and y-direction in a recursive manner. Each stretch keeps the line segments already on the square lattice on the lattice, but takes at least one line segment on a red-red edge path that is not on the square lattice to the lattice.

We need to be careful to not disturb the existing blue squares and red rectangles by these stretches. If a blue square is intersected by a line t that contains a segment of a red-red edge then we first move the blue square slightly to ensure that t cuts edges in the blue square only transversely. Next the lattice line is inserted at t which stretches one side of the blue square to a length of $t + 3\ell$. The blue square is reconstructed inside this rectangle with side length 3ℓ without intersecting t. See Figure 20 for an illustration of this. If a red rectangle is intersected by a line t, adding the lattice line results in a red rectangle which still satisfies the required size restrictions and no additional steps must be taken.

Furthermore, the red rectangles remain disjoint and the blue triangles still share no common x- or y-coordinates after the stretches. It is easy to see that this is always possible. The resulting graph is denoted by H^g. This process does not change the structure of the blue bands, it only moved some blue squares with their corresponding blue bands and blue vertices by a rigid motion. Thus the graph H^g satisfies all the conditions of a grid-like embedding. □

6.2. Grid-like embedding via re-connection. Using a recursive subdivision process of G to construct a grid-like embedding of G on the lattice requires a procedure to combine two grid-like embeddings of BRT-graphs (obtained from either a circular edge-cut or a vertex-cut subdivision) into a new grid-like embedding. More precisely, let $G_0 = G(i, j)$, $G_1 = G(i+1, 2j-1)$ and $G_2 = G(i+1, 2j)$ be three BRT-graphs obtained in the subdivision process of G by a vertex-cut subdivision or an edge-cut subdivision as defined in the paragraph after Definition 4.5. We assume that for $i = 1, 2$, G_i has a grid-like embedding G_i^g embedded in a box B_i, which has the rectangle R_i as its base in $z = 0$ and the height t_i. In addition, we assume the following convention: if $G_0 = G(i, j)$ was divided using a circular edge-cut, then G_1 refers to the BRT-graph which is derived from the graph inside γ'; if $G(i, j)$ was divided using a vertex-cut, then G_1 refers to the subgraph which contains the maximal disk-components mentioned in 4.4 (ii), or if the balanced vertex cut is chosen following 4.4 (i) it refers arbitrarily to any one of the two subgraphs.

This section describes a procedure to obtain a grid-like embedding G_0^g of $G(i,j)$ using only information from the given embeddings G_1^g and G_2^g and from the gluing instruction $N(i,j)$. During the description, we refer to the blue vertices $v^b(i+1, 2j-1)$ and $v^b(i+1, 2j)$ created by the subdivision as v_1^b and v_2^b, respectively.

We split the construction into 7 steps. Steps (1) through (3) serve to prepare the graphs G_1^g and G_2^g for the connection process, while steps (4) through (7) make the actual connection of the edges.

(1) Align the boxes B_i containing the G_i^g properly in the x- and y-directions next to each other, with their base rectangles in the plane $z = 0$. Without loss of generality we assume that the space between the two boxes is exactly one unit in the x-direction and that one side of the boxes coincides with the x-axis. Furthermore all the red squares and all the red-red edges outside the red rectangles are still on the cubic lattice. In the gap between the boxes we put a *connecting rectangle* at height $z = t_c = \max\{t_1, t_2\}$. The connecting rectangle has dimensions $1 \times y$ where $y = \max\{y_1, y_2\}$ and y_i is the y-dimension of the box B_i in their new location, see Figure 14.

(2) Create a (rectangular) box B_0 which includes both boxes B_1 and B_2 and the connecting rectangle and is of height $t_0 = t_c + 1$.

(3) Extend the blue vertices in G_1^g and G_2^g other than the v_i^b to the top of the box B_0 by extending their blue bands vertically by one unit and also lifting the blue triangles vertically by one unit.

(4) Delete the blue triangles at the blue vertices v_1^b and v_2^b and extend the corresponding blue bands in the z-direction to the plane t_c. Then extend the blue bands horizontally in the plane $z = t_c$ to the connecting rectangle. We refer to this horizontal extension of the blue band as the *extension band*. The two extension bands and the connecting rectangle is referred to as the *connecting strip*. The extension band consists of rectangles in the plane $z = t_c$. It starts in the direction of the extension vector in the case of circular edge-cut and in the opposite direction of the extension vector in the case of vertex-cut. With at most two right angle turns within $S \times \{t_c\}$ (where S is the blue square of the corresponding blue vertex), it can be made moving toward the connecting rectangle. With two right angle turns in the connecting rectangle and a suitable bandwidth change, it is then connected to the extension band coming from the other blue vertex, see Figure 14 (which is a case of the circular edge-cut subdivision). Since the turns only happen in the connecting rectangle and in the blue squares (at the $z = t_c$ level), the projection of the extension band into the xy-plane does not intersect any other blue square (hence itself will not intersect any other blue band in the rectangular boxes B_i). This is true because of the properties of the blue squares and blue bands.

(5) This step applies when G_1 and G_2 are obtained after a circular edge-cut subdivision, so the extension band starts in the direction of the extension vector. Recall that we had assumed that in this case G_1 is the BRT-graph inside γ'. So v_1^b is clockwise and v_2^b is counterclockwise, see the paragraph marked as "Orientation

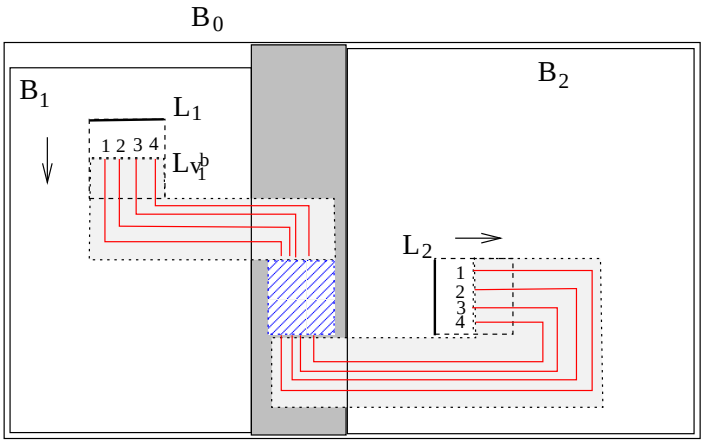

FIGURE 14. The top view of the boxes B_0, B_1, B_2 and the connecting rectangle (shaded rectangle in the middle) in the case that the blue vertices are created by a circular edge-cut subdivision. Several typical paths from the top of a blue band to the other blue band are shown as well, with the labels of the edges to show how the corresponding edges should line up on the opposite sides of the connecting rectangle. Only the center parts of the blue squares are shown and they are greatly enlarged to reveal the details.

determination" before Definition 5.1. Cut the neighborhood $N(i,j)$ open along β and stretch it into a rectangle called $N'(i,j)$ as we did in Figure 5. Modify and re-scale $N'(i,j)$ so that (a) its side lengths are smaller than one third of the side lengths of either of the two blue squares and (b) each path connecting two opposite boundary points that correspond to the intersection points of the same edge with $\partial N(i,j)$ is just a single line segment (parallel to either the x- or the y-axis). This rectangle is then placed into the connecting rectangle and is denoted by N''. Since the linear order of the edges along the extension band is the same as the linear order of v_1^b (and v_2^b) by the definition of grid-like embedding and the fact that G_1 and G_2 are grid-like embeddings. Thus edges with the same labels (edges that are to be connected) from each side (namely either from the G_1 or G_2 side) can be aligned perfectly with their counter parts of the edges of N'' as shown in Figure 15.

This connects all the edges in the blue bands and their extension bands arising from G_1^g and G_2^g. In particular, an edge from G_1^g is connected to an edge G_2^g only if both edges have the same label and no additional crossings are introduced. By our construction, these edges consist of only straight line segments. In particular any edge passing from the extension band of G_1^g to the extension band of G_2^g contains only two right angle turns on the connecting rectangle.

$N'(i,j)$ may contain one or more new blue vertices. For each such blue vertex u, extend each edge connected to u from where it enters N'' to the centerline of N'', then extend it up by one unit. Create a small blue square in $z = t_c + 1$ over

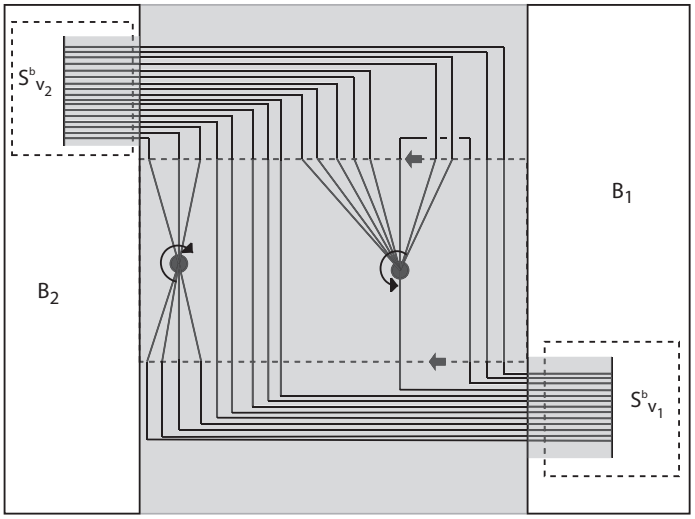

FIGURE 15. How G_1 and G_2 are reconnected: The connecting rectangle is made much wider to show the details. In the middle of the connecting rectangle is N'', which is a deformation of the neighborhood of Figure 5. The curve that went under two edges represents a loop edge deleted when G_1 and G_2 were created.

N'' for this blue vertex. Then a blue band, and a blue triangle with the new blue vertex on top of the blue triangle in the plane $z = t_c + 2$, following the same rules as before (for grid-like embeddings). See Figure 16.

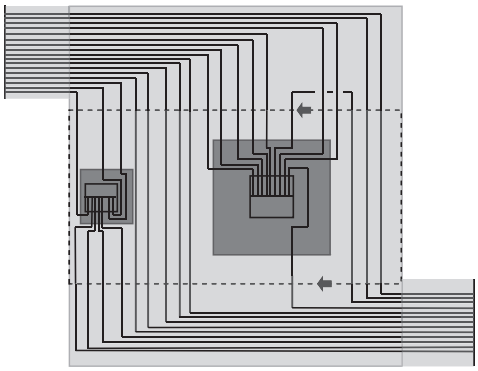

FIGURE 16. The edges on the connecting rectangle of Figure 15 are grid-like and two new blue squares with blue bands and triangles have been created. The Figure is not to scale and the new blue squares appear to be much larger than they actually are. The linear orders at the new blue vertices are recovered from their corresponding gluing instructions. Only the top view is shown so the new blue vertices and blue triangles are not visible in the figure.

Since the size of the new blue squares can be arbitrarily small and each blue vertex in N'' has certain free space to move (without crossing the straight paths that have been placed), the projections of the blue squares to the x- and the y-axes can be adjusted so as not to overlap with each other or with any other existing blue squares. For each blue square, the edges are combined into a vertical blue band as before and topped with a blue triangle at $z = t_c + 1$. At this point all edges that are connected to v_1^b or v_2^b are accounted for.

Note that we have not addressed the labels on $N(i, j)$ that correspond to loop edges that were deleted from G_{1l} and G_{2l} when G_1 and G_2 were created (although one such edge has been illustrated in Figure 16). We will address this in Step (6).

(5′) This step applies when G_1 and G_2 are obtained after a vertex-cut subdivision. For the vertex-cut, v_1^g and v_2^g have the same orientations in the plane. Since the extension band in this case starts in the direction opposite to the orientation vector, the linear orders of the edges along the band sides will again align correctly. See Figures 17 and 18 for an illustration of this.

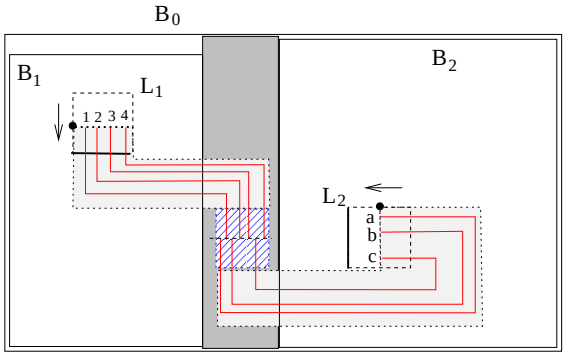

FIGURE 17. Top view of an example for case 5′. In this case the original linear order of the edges at the blue vertex v_0^b is $a1b23c4$. The solid dots can be thought of as the point β used to define the linear order. A simplified 3D view of this is shown in Figure 18.

The connecting rectangle contains $N(i, j)$ with a single blue vertex v_0^b that was split into the two blue vertices v_1^b and v_2^b. As in the case of an edge-cut, a blue square is created in $z = t_c + 1$ first, then a blue band, and a blue triangle with the new blue vertex on top of the blue triangle in $z = t_c + 2$, satisfying all requirements of a grid-like embedding. This connects all the edges in the extension bands originated in the blue bands $B_{v_1^b}$ and $B_{v_2^b}$. Notice that the linear order of the edges at v_0^b is restored when the edges from two sides meet the middle bar of the connecting rectangle.

(6) This step deals with the loop edges deleted after a circular edge-cut subdivision (such deletion can only happen in the case of a circular edge-cut subdivision). In the case that G_1 and G_2 are obtained after some loop edges are deleted, then

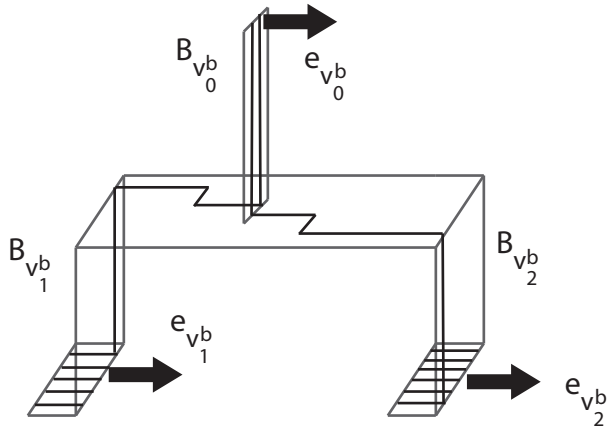

FIGURE 18. Shown are the three blue bands $B_{v_1^b}$, $B_{v_2^b}$, and $B_{v_0^b}$ (in gray) together with the three extension vectors $e_{v_1^b}$, $e_{v_2^b}$, and $e_{v_0^b}$ that arises in a vertex cut. The connection is only shown schematically without horizontal turns and the width of the bands is not to scale. Only two edges (black) are shown to illustrate the layout.

$N'(i,j)$ contain labels not used to G_1^g and G_2^g. The creation of temporary loop edges can happen in two ways.

The first case is when a red-red edge e (not on γ) was cut twice by γ'. Both red vertices incident to e are contained in one of the graphs, say in G_1 (the case if the vertices are contained in G_2 is identical) and therefore in G_1^g. The middle arc of e is contracted into a loop in G_2' and is eventually deleted. This leads to 4 identical labels on $\partial N(i,j)$, two each on each component of $\partial N(i,j)$. Two labels in one boundary component of $\partial N(i,j)$ are accounted for by their corresponding edges on the extension band originated from $B^b_{v_1^b}$. The other two labels on the other boundary component of $\partial N(i,j)$ have no corresponding labels on v_2^b. The two edges coming up from G_1^g just end on the opposite side of N'' (and there will be no other edges with the same label later on to connect them). However this is no problem since the gluing instruction tells us that these two edge ends must be connected to each other at this stage. Usually, this cannot be done in the plane t_c without creating crossings. The connection is made using five edge segments, three of which are in the plane $t_c - 1$. Both edges are extended to the end of the connecting rectangle, see Figure 16 for an example of such an edge. A vertical segment of unit length is added at the end of each of the edges, connecting the plane at level t_c with the plane at level $t_c - 1$. A short segment parallel to the y-axis is added to the ends of both vertical segments and then one segment parallel to the x-axis connects the two end points. This construction builds a small 'hook' which hangs below the connecting rectangle. Several such loops may have been removed during a subdivision step. For each of them a hook creates the correct

connection between the edges without adding unwanted crossings. Loops may be nested, and the hooks can be nested too. A higher nesting level of the loops leads to slightly longer pairs of parallel segments which are parallel to the y-axis and a longer horizontal segment parallel to the x-axis.

In the second case, a red-blue edge (not on γ) connected to the same blue vertex v not on γ are cut once by γ'. If there is just one such edge then this edge is contracted and does not lead to a loop. However if there is more than one, only one is contracted and the others result in loops. Let e be one such edge. Then the red vertex connected to e is contained in one of the graphs, say in G_1 (the case if the vertex is contained in G_2 is identical) and therefore in G_1^g. The part of e connected to the blue vertex is contracted into a loop in G'_{2l} and was deleted. This leads to 3 identical labels on $\partial N(i,j)$, one on the boundary component belonging to G_1 and the other two on the boundary component belonging to G_2. The single label in one boundary component of $\partial N(i,j)$ is accounted for by by a corresponding label of edges on the extension band originating from $B^b_{v_1^b}$. The two labels on the other boundary component of $\partial N(i,j)$ are not accounted for by corresponding labels on edges connected to v_2^b. We now construct a 'small' hook exactly as in the first case.

Notice that the loops in G'_{1l} and G'_{2l} are positioned at different ends of the neighborhood rectangle, that is, the end that is closer to B_1^b and B_2^b, respectively. The loops on each side nest perfectly but the loops on both sides combined may not exhibit a nesting behavior. After this step the connecting rectangle contains edges accounted for all labels on $N(i,j)$ and in the same arrangement as is specified in $N(i,j)$.

(7) This last step only applies to the case when G_1 and G_2 are obtained after a circular edge-cut subdivision. The reason is in this case, we may have created red-red edges that are no longer on the lattice hence the reconnected graph described in the earlier steps is not grid-like yet. We will remedy this problem by adding new gridlines in the x- and y-direction to put newly formed red-red edges on lattice. For each line segment (on the re-connected red-red edge) parallel to the y-axis, a new x-gridline is added (which corresponds to a stretching isotopy). For each line segment parallel to the x-axis, a new y-gridline is added. See Figure 19.

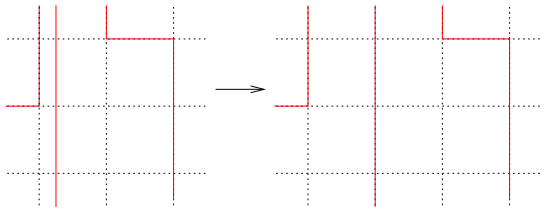

FIGURE 19. Stretching the space to accommodate a newly created red-red edge on the lattice.

In this process we destroy the blue squares that formerly belong to the now vanished blue vertices v_1^b and v_2^b. These blue squares are no longer needed. All other blue squares must be preserved. If one of these new gridlines hits the projection of a blue square S_v^b then we need to adjust the blue square as follows, see Figure 20. First we slightly move the blue square to make sure that the new gridline hits edges in the blue square only transversely. Then we expand the blue square as is required by the insertion of the new grid line. The expanded S_v^b now becomes a rectangle with one of its sides having a length of more than one unit. In this rectangle we put a copy of the original center square R_v with the original small width ℓ by translation. (If we inserted an x- or y- gridline then we translate R_v in x- or y-direction, respectively.) This can be connected up with exactly an many turns for the edges as before. Around this newly positioned square R_v we reposition an new blue square S_v^b with the original size. By default this new blue square has a projection that is disjoint in x- and y-coordinates from the projections of all the other blue squares.

If one of these new gridlines hits a red rectangle then we simply stretch the red rectangle into a larger rectangle. This does not introduce any new turns and preserves all the required properties of a grid-like embedding.

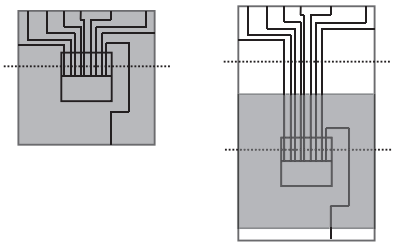

FIGURE 20. On the left a blue square with a needed new gridline (dashed). On the right the blue square has been expand by one unit in the y-direction without creating any additional turns. The original center square R_v has been translated in y-direction and a new blue square of the same size as the original has been created with R_v at its center. The Figure is not to scale and the new blue squares appear to be larger than they are.

This completes the description of how to combine the two grid-like embeddings of G_1 and G_2 into a new grid-like embedding of G_0.

7. The Verification of Topology Preservation

While a grid-like embedding of a BRT-graph obtained as given in Lemma 6.1 preserves its topology by its construction, it is far from obvious that the embedding obtained by reconnecting two grid-like embeddings as given in Section 6.2 preserves the topology of the original BRT-graph from which the two grid-like embeddings are induced. We will prove that this is indeed the case in this section.

Lemma 7.1. *Let $G_1 = G(i+1, 2j-1)$ and $G_2 = G(i+1, 2j)$ be BRT-graphs obtained from the BRT-graph $G_0 = G(i,j)$ by a subdivision. Then the grid-like embedding G_0^g of G_0 as described in Section 6.2, confined in a rectangular box of the form $R_0' \times [0, t_0]$, is isotopic to $G(i,j)$ by a VNP-isotopy that is the identity outside a small neighborhood of the box $B_0' = R_0' \times [-1, t_0 - \delta]$. Therefore, G_0^g is indeed a grid-like embedding of G_0 since it satisfies all other requirements of a grid-like embedding of G_0.*

Before stating the proof, let us recall that G_1 is either the interior graph in the case of a circular edge-cut subdivision, or the graph containing one disk-component or a union of some maximal disk-components in the case of a vertex-cut subdivision.

PROOF. All the requirements for a grid-like embedding of $G(i,j)$ as specified in Definition 5.4 are already satisfied by the construction process outlined in Section 6.2, as one can check. Thus it suffices to show that the grid-like embedding obtained is isotopic to a standard 3D-embedding of G_0.

In the last step in the construction process described in Section 6.2, the box B_0 (and the boxes B_1 and B_2) are stretched to make room for new gridlines so that the newly created red-red edges can be put on the lattice. Let us call the stretched boxes B_0', B_1' and B_2'.

Case 1: The case of a circular edge-cut subdivision. The VNP-isotopy will be constructed by a sequence of isotopies using the following steps:

(1) Remove some gridlines to get back to an almost grid-like embedding;

(2) Shrink B_1' and B_2' (with the graphs contained in them) back to B_1, B_2 and deform the graphs contained in them to 3D standard embeddings;

(3) Deform the hooks (representing the loop edges that were deleted during the subdivision) from the connecting rectangle into the plane $z = 0$;

(4) Shrink G_1 and drag the shrank G_1 along the extension bands and the connecting rectangle and drop it into G_2 on $z = 0$.

(5) Straighten out the blue squares and make the blue-bands vertical as required by a standard 3D-embedding of G_0 using Lemma 2.5.

We now address each of these points in detail.

(1) Clearly such stretching isotopies are reversible. However the definition of a grid-like embedding does not allow us to use an isotopy that changes the entire box B_0. Thus we can only shrink the box B_0' (together with B_1' and B_2') back to its original size under $z = t_0 - 2 = t_c$. The first isotopy is defined by this shrinking isotopy ϕ' for $z \leq t_0 - 2$, the identity for $z \leq -1$ and $z \geq t_0 - 1 - \delta$ where $\delta > 0$ is the number chosen so that all blue triangles have bases on $z = t_0 - 1 - \delta$. Let f be a blue band at a blue vertex v. f intersects the base of its corresponding blue triangle at b and intersects the plane $z = t_0 - 2$ at c. Let c' be the image of c under ϕ'. Then the isotopy for $t_0 - 2 \leq z \leq t_0 - 1 - \delta$ is chosen so that the part of f between b and c (which is a vertical band) is mapped to the band joining b and c'

(which may no longer be a vertical band). This can be done since the shrinkage ϕ' on $R_0 \times \{t_0 - 2\}$ (R_0 is the base of B_0) will not cause these bands to intersect each other by the conditions on the positions of the blue squares. This isotopy restores the original boxes B_1 and B_2 together with all the blue squares. The blue triangles in B_0' remain the same, the vertical blue bands from $z = t_0 - 1$ to $z = t_0 - 2$ are no longer vertical (however they remain disjoint from each other and are strictly increasing in the z-coordinates). The part of a blue band under $z = t_0 - 2$ remain vertical after this isotopy is applied.

(2) After isotopy (1) the graphs G_1 and G_2 fit back into the original B_1 and B_2. The resulting embeddings "almost" restore G_1^g and G_2^g. The "almost" stems from the exception that the blue triangles in each box that would be part of a grid-like embedding are distorted, however they are identical to G_1^g and G_2^g below the z-level where the bases of their blue triangles are. By a slight abuses of notation we call these "almost" grid-like embeddings still G_1^g and G_2^g. By the definition of grid-like embedding, G_1^g (G_2^g) is isotopic to a standard 3D-embedding G_1^s (G_2^s) by a VNP-isotopy that is identity outside the box $R_1 \times [-1, t_1 - \delta]$ ($R_2 \times [-1, t_2 - \delta]$), see Definition 5.4 (v). We will now apply these two isotopies to G_1^g and G_2^g. After this, an edge path from the base rectangle R_0 to a blue vertex already existed in G_1^g and G_2^g before the reconnection consists of four straight line segments: a single vertical line segment from R_0 to $z = t_0 - 2$, then a line segment (that is in a deformed blue band) from $z = t_0 - 2$ to $z = t_0 - 1$, then a vertical line segment from $z = t_0 - 1$ to the base of a blue triangle in $z = t_0 - \delta$, followed a line segment in a blue triangle leading to the blue vertex. Notice that the last two line segments are not changed by the isotopy applied so far. Note also that these paths do not intersect the connecting rectangle (which is also not affected by the last two isotopies since it is in $z = t_c = t_0 - 2$). See Figure 21.

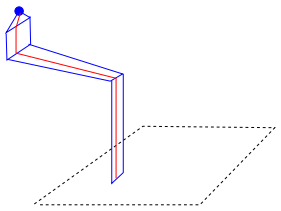

FIGURE 21. An edge path from the base rectangle R_1 (or R_2) to a blue vertex after the isotopy in (2) is applied to the grid-like embedding G_0^g constructed from G_1^g and G_2^g.

(3) During an edge-cut it is possible that in the contracting process we created temporary loop edges that were deleted in order to form G_1 and G_2. These loop edges are realized by some "small hooks" that are attached at the two ends of the neighborhood rectangle on the connecting rectangle (N'') below $z = t_0 - 2$ in the reconnecting process (Step (6) of Section 6.2). At this stage we must realize these

loops in the plane $z = 0$ as it is required in a standard 3D-embedding of G_0. A top view of two nested such hooks and their relative positions with the other edges involved in the same blue square (on $z = 0$) are illustrated in Figure 22.

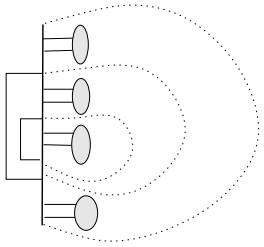

FIGURE 22. A top view of two nested hooks and their relative positions with the other edges involved in the same blue square: the thick line segment represents the segment L used in a blue square, the large outside dashed curve is a conceptual depiction of the deformed γ', the two small dashed curves represent the actual loops corresponding to the two hooks.

We accomplish this one hook at a time starting with an innermost hook. We slide a hook along the blue bands down into the plane $z = 0$, see Figure 23. Once they are in the plane $z = 0$ we fold them by a 90 degree turn into the unused space in the blue square so they look just as shown in Figure 22. It is clear from the figure that the hook can then be deformed to the dashed curves from under the plane $z = 0$ by a VNP-isotopy that is identity below $z = -1$. Of course it needs to remain in the box B_i to which it belongs. See Figure 23 for an illustration of this process.

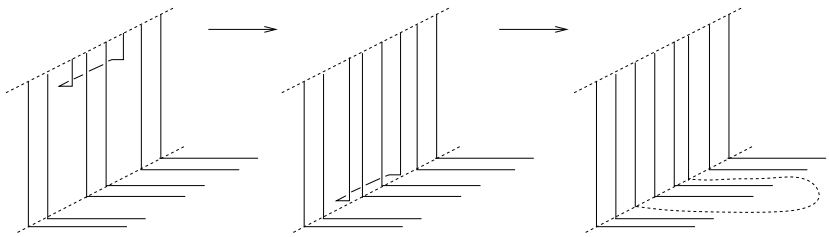

FIGURE 23. How a small hook (loop) is isotoped along a blue band into the plane $z = 0$. The edge on the right is dashed because it might have to be stretched out to fit into the plane $z = 0$ and can be quite long.

(4) Let us recall that at this point all red vertices are in the plane $z = 0$ and all blue vertices are in the plane $z = t_0 + 2$. Also, all the red-red edges are also in the plane $z = 0$ except those going through the connecting strip (created in the

re-connecting process). We cannot simply project these into the plane $z = 0$ since that will likely to create crossings so we will not be able to recover our original plane graph this way. Since we know that the edges connected to v_2^b in B_2 are in the outer face of G_1, we will try to shrink the graph G_1 first and then move the whole graph along the connecting strip into the interior face F of G_2 where it becomes clear that the original graph structure is recovered. The blue bands remain connected to the top of the box B_0. In this way we avoid the creation of unwanted intersections. In the following we describe these steps in more detail.

Assume that w_1, w_2, ..., w_k are the centers of the blue squares associated with the blue vertices in G_1^g other than v_1^b. Let R_s be the half of the square $R_{v_1^b}$ in the center of the blue square $S^b_{v_1^b}$ between L_1 and $L_{v_1^b}$ as shown in Figure 25. Choose k points y_1, y_2, ..., y_k in the small rectangle R_s such that the y_j's do not share the same x-coordinates nor y-coordinates. This small rectangle can be viewed from the top as the rectangle with dotted line boundary and the letter G_1^s as marked in Figure 25. By Lemma 2.3, there exists a plane isotopy $\xi : R_1 \times [0, 1] \to R_1$ that is identity outside a small neighborhood of R_1 and the identity on $L_{v_1^1}$ (the base of the blue band) that takes w_j to y_j and moves the all points of the embedding G_2^s in the plane $z = 0$ into R_s. Here we assume that $\xi_0 = \xi(x, 0)$ is the identity on R_1 and $\xi_1 = \xi(x, 1)$ has moved all the w_j's to the y_j's. This plane isotopy is extended to a VNP-isotopy in the following way: (a) it is the identity outside of the box $R_1 \times [-1, t_1 - 1/2]$; (b) its action on $R_1 \times \{s\}$ for each $0 \le s \le t_1 - 1/2$ is the same as that of $\xi(x, m(1 - s/(t_1 - 1/2)))$ for $m \in [0, 1]$ on $R_1 \times \{0\}$. Note that this extension keeps all blue bands disjoint from each other and each edge on a blue band is a path that is non-decreasing in the z direction. Furthermore, the isotopy can be so chosen that the bases of the blue bands are mapped to bands perpendicular to the direction of the extension vector. See Figure 24.

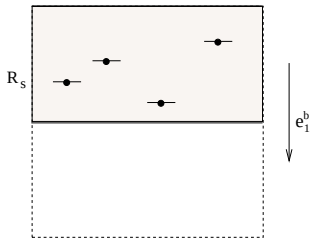

FIGURE 24. How G_1^g looks after it is shrank to fit in R_s. The dots are the blue vertices and the bars on them indicate the bases of the blue squares after the isotopy.

We now define an isotopy that retracts the connecting strip while dragging the rectangle R_s with the edges of G_1 along the connecting strip. At first, the rectangle R_s containing G_1 can be lifted vertically to the level $z = t_c$. In doing so we retract the connecting strip at the same time. All the blue bands that are connecting R_s

to the blue vertices at the top of the box B_0 are deformed as well to keep the bands nondecreasing in the z-coordinates. An illustration of this process is shown in Figures 25 and 26. This isotopy clearly preserves the neighborhood structures of the vertices.

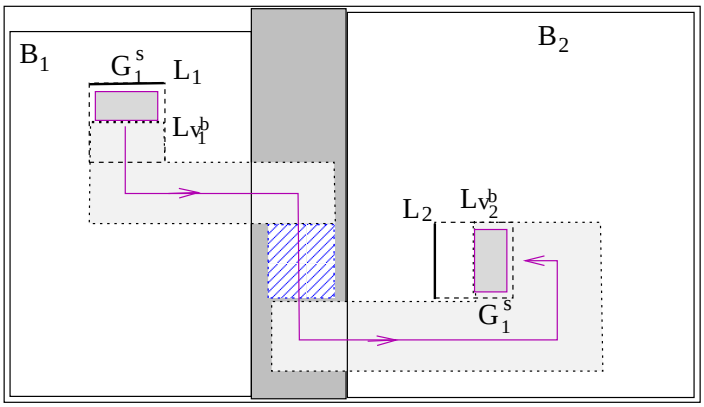

FIGURE 25. Shrinking G_1 and moving it to the unused space in the blue square at v_2^b.

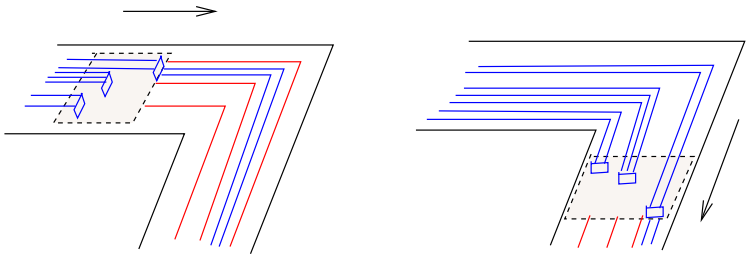

FIGURE 26. Two middle steps of the "dragging" isotopy: the graph is in the gray area and not explicitly shown to keep the drawing simple. The blue band on the boundary of R_s corresponds to a blue vertex recovered in the reconnection process.

The retraction continues along the horizontal parts of the extension bands and the connecting rectangle. Whenever the connecting strip turns horizontally we turn the whole rectangle R_s accordingly. Again all the blue bands that are connecting R_s to the blue vertices at the top of the box B_0 are dragged along and kept as increasing in their z-coordinates as shown in Figure 26. At the end of the extension band that leads into B_2 it is time to drop the small rectangle containing G_1 vertically down. By our assumptions on the extension vector at v_2^b, there is free space in the small rectangle $R_{v_2^b}$ in the blue square $S^b_{v_2^b}$ to put the box R_s into the

plane $z = 0$. Once the small rectangle R_s is in the plane $z = 0$ the connecting strip has been completely eliminated. We now have the graph $G_0 = G(i, j)$ embedded into the plane $z = 0$ with the exception of the blue vertices of G_0. For each blue vertex there is a small blue square (the blue squares have different sizes) and a blue band that connects the blue square to a blue vertex on the top of B_0 along a path that is non-decreasing in the z direction. Since we can deform the blue vertices (with the edges connected to them) into the plane $z = 0$ along the deformed bands one by one without any interference and without crossing the boundary of $R_{v_2^b}$, it is clear that the resulting graph bounded within $R_{v_2^b}$ is topologically equivalent to G_1 and the resulting graph outside $R_{v_2^b}$ is topologically equivalent to G_2. These two graphs are connected along the boundary of $R_{v_2^b}$ following the gluing instruction. Thus the graph obtained after the reconnection is indeed isotopic to G_0.

(5) Now let p_1, p_2, ..., p_j be all the intersection points of the edges leading out from the blue vertices of G_0^g with the bases of the blue triangles in B_0 (they are all in the plane $z = t_0 - \delta$) and let q_1, q_2, ... q_j be the first intersection points of the corresponding edges with the plane $z = 0$. By our construction, p_i and q_i are connected by a path that is non-decreasing in the z direction and these paths do not intersect each other. By Lemma 2.5 and Remark 2.6 after it, there exists a VNP-isotopy Ψ such that Ψ is the identity in $z \geq t_0 - \delta$ and outside a small neighborhood of B_0, and Ψ deforms each path connecting p_i to q_i to a straight line segment and Ψ is a plane isotopy when restricted to $z = 0$. The edges in $z = 0$ can be further deformed to create spaces for the required blue squares in $z = 0$. The result is the desired standard 3D-embedding of G_0. This finishes the proof of the first case.

Case 2: The case of a vertex-cut subdivision. The situation in this case is slightly simpler because no temporary loop edges are created and the connecting rectangle contains exactly one blue square $S^b_{v_0^b}$. Thus one of the steps in the prior isotopy is no longer needed. The isotopy is again constructed by a sequence of isotopies using the following steps:

(1) Remove some gridlines to get back to an almost grid-like embedding;

(2) Shrink B_1' and B_2' (with the graphs contained in them) back to B_1, B_2 and deform the graphs contained in them to 3D standard embeddings;

(3) Shrink G_1 and drag the shrank G_1 along the extension bands and the connecting rectangle and drop it into G_2 on $z = 0$.

(4) Straighten out the blue squares and make the blue-bands vertical as required by a standard 3D-embedding of G_0 using Lemma 2.5.

Note that it is essential that G_1 is used in step (4). For example, suppose we are in case (ii) of Lemma 4.4, that is G_1 consists of a union of several maximal disk-components of a single inseparable disk-component. Then it is possible to drag G_1 into G_2 in step (3) above, but it might not be possible to drag G_2 into G_1 without getting hung up on some blue band that is connected to the top of the box B_0.

Some more argument is needed for the isotopy in Step (4). In the case for the edge-cut, the shrunk graph G_1 is positioned in the unused rectangle in $R_{v_2^b}$ so placing G_1 into that space apparently will not cause of edge intersections. However, in this case the shrunk graph G_1 is positioned into the *used* half of $R_{v_2^b}$ in G_2. Since G_1 contains some (or all) maximal disk components of some inseparable disk component Q of G_0, the edges from G_1 connected to the blue band $B^b_{v_1^b}$ fit precisely between the edges of the $Q \setminus G_1$ in G_2 already connecting to $L_{v_2^b}$. If one combines Figures 18 and 26 (but without the red-red edges shown), then this becomes clearer.

The details of the isotopies are otherwise similar to the edge-cut argument and are thus left to the reader. This finishes the proof and also concludes this section. □

8. Embedding Length Analysis

One way to estimate the embedding length is to estimate the volume of the box B_0 in this construction. By our design of the construction, the height of B_0 is only two units larger than the maximum height of the two boxes B_1 and B_2. We can thus estimate the volume of B_0 by estimating the area of the base rectangle of B_0. One way to do this is to count the number of horizontal gridlines in the x- and y-direction we must create to accommodate a newly created red-red edge. A gridline is consumed either by a segment of the red-red edge in the xy-plane using that gridline or by the red-red edge moving through a vertical segment parallel to the z-axis. More precisely we are interested in the following. Let e be a newly created red-red edge and consider a vertical projection $p(e)$ of e into the xy-plane. We count the 90 degree turns of $p(e)$ and add to it the number of segments parallel to the z-axis to obtain an estimate on the number of gridlines that need to be available in the base rectangle R_0.

Definition 8.1. Let (G^g, B) be a grid-like embedding of a BRT-graph G contained in a rectangular box B. Let $E_{br}(G)$ be the set of red-blue edges in G. For any edge $e \in E(G)$ (e can be a red-red or a blue-red edge) denote with $tr(e)$ the number of different horizontal gridlines (in the x- and y-direction) needed and call this the *turning number* of the edge e. We define the *turning number* $T(G^g, B)$ of (G^g, B) as follows:

$$T(G^g, B) = \max_{e \in E_{br}(G)} \{tr(e)\}.$$

Note that in the above definition we ignore the turns which are not a 90 degree angle that may occur when an edge enters a red rectangle or a blue triangle. Counting the 90 degree turns in $p(e)$ over counts the gridlines needed for the horizontal segments in the red-red edge, since several segments of $p(e)$ may end up on the same gridline. Note also that $p(e)$ may have 180 degree turns that arise when two consecutive turns in the xz or yz plane occur, as is the case for a hook. Those are not counted, since the vertical segments are counted separately. We are now able to show the following Theorem.

Theorem 8.2. *Let G_1 and G_2 be the BRT-graphs obtained from the BRT-graph G_0 by a single subdivision (either a vertex-cut or an edge-cut). Let G_0^g be the grid-like embedding of G_0 in a rectangular box $B_0 = R_0 \times [0, t_0]$, obtained by reconnecting the grid-like embeddings G_1^g, G_2^g of G_1, G_2 as described in Section 6.2. If $T(G_1^g, B_1) = n_1$ and $T(G_2^g, B_2) = n_2$, then the grid-like embedding G_0^g of G_0 has the following properties:*

(i) For a newly constructed red-red edge e of G_0 $tr(e) \leq 2\max\{n_1, n_2\} + 8$.

(ii) $T(G_0^g, B_0) \leq \max\{n_1, n_2\} + 17$.

Proof. We first prove (i). Note that a newly constructed red-red edge can only appear if G_1 and G_2 are created by an edge-cut in G_0. The path a newly created red-red edge e travels is divided into three parts, where each part is a union of one or more line segments each of which is parallel to one of the coordinate axis. There are two cases to consider: the curve γ' (the push-off of γ as defined in Section 3) intersects e once or the curve γ' intersects e twice.

In the first case when traveling along the edge e we encounter the following parts: The first part starts at a red vertex, say in G_1^g, moves to the blue square $S^b_{v_1^b}$, and continues through the blue square to the base of the blue band $B_{v_1^b}$ and then up along the blue band. At this point we know that this first part of e has at most turning number n_1. The middle part of e begins with a 90 degree turn in the xz- or yz-plane, from the vertical direction on the blue band $B_{v_1^b}$ to the extension band, moves through the connecting strip and ends with a 90 degree turn (again in the xz- or yz-plane) from the horizontal extension band to the vertical direction on the blue band $B_{v_2^b}$. It takes at most 2 turns to reach the connecting rectangle from each box B_i and two turns to turn onto and off the connecting rectangle, giving us a turning number of at most 6 for the middle part. The two 90 degree turns off and onto the vertical blue band $B_{v_i^b}$ are not counted, since the need for this gridline is already accounted for when the blue band is created. Thus $tr(e) \leq n_1 + n_2 + 6$ in G_0^g.

If we assume that an edge $e = w_1w_2$ is intersected by γ' twice then both vertices w_1 and w_2 are in the same graph G_i. The middle part of e that does not contain any of the two vertices, is contracted into a loop edge and then deleted. In the reconstruction process a small hook is constructed whose projection looks like the letter H. The horizontal bar of the H is the edge segment of the hook in the xy-plane below the connecting rectangle which is not connected to a vertical segment and one gridline needs to be added for it. One pair of ends of the two parallel lines in the H is connected to w_1 and w_2, the other pair of ends is connected to the vertical segments of the constructed hook. Since both ends are on the same line (in the x- or y-direction) only one gridline needs to be added even though there are two vertical segments. We account for the fact that both w_1 and w_2 are in the same graph by using a maximum. In this case the turning number satisfies $tr(e) \leq 2\max\{n_1, n_2\} + 8$ turns in G_0^g.

Next we prove (ii) by proving that $tr(e)$ for a red-blue edge e is $\leq \max\{n_1, n_2\}+16$. We consider the case of an edge-cut first. Let e be a red-blue edge and assume that the red vertex w of e is contained in G_1^g (the case of G_2^g is accounted for by using a maximum as before) and that x is the blue vertex of e. We note that the curve γ' can intersect e at most once. The result of the edge-cut is a red-blue edge in G_1^g from w to the blue vertex v_1^b and potentially a deleted loop edge in G_2 that results in a hook in G_0^g. No loop (and thus no hook) is created if the blue vertex x is on γ', or if x is in G_2 and is not connected to any edge other than e which is cut by γ'.

First let us consider the case when there is no hook in G_0^g. In this case, e consists of two parts in G_1^g. As before, the first part starts at the red vertex w in G_1^g, moves to the blue square $S^b_{v_1^b}$, and continues through the blue square to the base of the blue band $B_{v_1^b}$ and then up along the blue band. This part contains at most n_1 turns. The second part of e begins with a 90 degree from the blue band $B_{v_1^b}$ to the extension band, moves through the extension band, onto the middle section of the connecting rectangle with at most 3 turns, then moves up to the new blue square with at most 4 more turns, once in the blue square, it may need up to another 6 turns to be re-routed to enter the middle square of the blue square in the correct order (to achieve the desired linear order), then finally move up to the base of the new blue triangle with one more turn. This part of the path will add at most 15 right angle turns for the second part (and 14 total) in this case.

In case there is a hook, more turns are needed for the second part. As before, the edge turns from the blue band onto the extension band, moves through the extension band, across the connecting rectangle, runs through the small hook, returns to the middle section of the connecting rectangle and then move up a level to a new blue square and finally to the base of a blue triangle. ends in one of the blue vertices w_{c_i} of G_0^g on the connecting rectangle. The extra number of gridlines needed for the loop is 2, as already established during our earlier discussion for the red-red edges. Thus $tr(e) \leq \max\{n_1, n_2\} + 17$ for an edge-cut.

We now consider the case of a vertex-cut. Here the situation is easier since the red-blue edge e is not cut into parts at all. It already exists in one of the two graphs G_i^g, $i = 1, 2$ and it is simply extended from the blue band $B_{v_i^b}$ to the single blue vertex v^b on the connecting rectangle. It is easy to see that this extension does not exceed 17 turns and thus the results from the edge-cut case suffices as an upper bound for $tr(e)$. □

We are now ready to prove the main theorem of this paper as stated below.

Theorem 8.3. *Let G be a 4-regular plane graph with n vertices. Then there exists a realization of G on the cubic lattice $\mathbb{Z}^3$ which is contained in a rectangular box whose volume is bounded above by $O(n \ln^5 n)$. Consequently, the ropelength of any knot or link K is at most of the order $O(Cr(K) \ln^5(Cr(K))$, where $Cr(K)$ is the minimum crossing number of K.*

To prove the theorem, we will use the non-linear recurrence analysis approach as described in [**17**]. The result of Theorem 8.2 and the results from the earlier sections will be needed when we apply this analysis.

For any rectangle R under discussion we assume that its length l is greater or equal to its width w. The *aspect ratio* σ of the rectangle R is defined by $\sigma = w/l$. From this it follows that $l = \sqrt{A/\sigma}$ and $w = \sqrt{\sigma A}$ where A is the area of the rectangle R. The aspect ratio is important to us because throughout the algorithm we want to operate with boxes whose base rectangles are not too skinny, that is the rectangles have an aspect ratio that is bounded away from zero by a positive constant.

In the previously described divide-and-conquer algorithm we divide a given BRT-graph at each step into subgraphs (also BRT-graphs) each of which has a size of at least 1/6 of the previous graph, where the size is measured by the number of red vertices in a graph. This allows us to operate with rectangles whose aspect ratios are at least 1/6. Before getting started on the details we need a preliminary lemma that asserts that we can divide rectangles while preserving the minimal aspect ratio of 1/6.

Lemma 8.4. *Let R be a rectangle with length l and width w and aspect ratio $\sigma = w/l \geq 1/6$. Let $1/6 \leq \alpha \leq 5/6$ be a real number and divide the rectangle R by a line that is parallel to its width into two rectangles R_1 and R_2 of areas αwl, $(1-\alpha)wl$ and aspect ratios σ_1, σ_2 respectively, then $\sigma_i \geq 1/6$ for each i.*

Proof. It suffices to show this for one of the aspect ratios, say σ_1 of the rectangle R_1. We can assume that the area of $R_1 = \alpha wl$ with dimensions αl and w. There are two cases to consider, either $w \geq \alpha l$ or $w < \alpha l$. If $w \geq \alpha l$ then $\sigma_1 = \alpha/\sigma$ and $1/6 \leq (1/6)/\sigma \leq \alpha/\sigma = \sigma_1$. If $w < \alpha l$ then $\sigma_1 = \sigma/\alpha$ and $1/6 < (1/6)/\alpha \leq \sigma/\alpha = \sigma_1$. □

From the previous sections we know that a BRT-graph G with n red vertices has a balanced recursive subdivision sequence whose depth is bounded above by $c_r \ln(n)$ for some constant $c_r > 0$, see Theorem 4.6. At the end of the subdivision process we have terminal BRT-graphs $G(i,j)$ that satisfy $W_s(G(i,j)) < W_0$. That is, each such terminal BRT-graph has less than W_0 red vertices. By Lemma 4.2, the number of blue vertices in $G(i,j)$ is bounded above by $3W_0$ (since the g used in Lemma 4.2 is equal to 12). Thus all graphs $G(i,j)$ have at most $n_0 = 4W_0$ vertices (blue and red combined). Since there are only finitely many plane BRT-graphs with at most W_0 red vertices and whose maximum vertex degree is 12 or less, the following lemma holds for a grid-like embedding $G^g(i,j)$ of a terminal BRT-graph $G(i,j)$.

Lemma 8.5. *There exists an integer $N_0 > 0$ such that if $G(i,j)$ is a terminal BRT-graph (so it has less than W_0 red vertices) and R is any rectangle of area $\geq N_0$ with an aspect ratio $\sigma \leq 1/6$, then R is large enough such that the rectangular box $B(i,j)$ of height 1 with R as its base rectangle can be used to hold a grid-like embedding*

$G^g(i,j)$ of $G(i,j)$. Moreover there exists a constant $m > 0$ that only depends on W_0 such that for any such grid-like embedding $G^g(i,j)$ in the box $B(i,j)$, the turning number $T(G^g(i,j), B(i,j)) \leq m$.

Let us now examine what happens in the reconstruction process. Let i_0 be the depth of the subdivision sequence. Recall that when two grid-like embeddings are reconnected, the turning number of a red-blue edge that remains a red-blue edge increases by at most c_t for some constant c_t (c_t can be chosen to be 17 in fact, see Theorem 8.2 (ii)).

Therefore if a grid-like graph $G^g(i_0 - 1, j)$ is reconstructed from the grid-like embeddings $G^g(i_0, 2j-1)$ and $G^g(i_0, 2j)$ in a box $B(i_0 - 1, j)$, the height of $B(i_0 - 1, j)$ is $1 + 2 = 3$ and $T(G^g(i_0 - 1, j), B(i_0 - 1, j)) \leq m + c_t$. Inductively, we can see that if a grid-like graph $G^g(i,j)$ is reconstructed from the grid-like embeddings $G^g(i+1, 2j-1)$ and $G^g(i+1, 2j)$ in a box $B(i,j)$, then the height of $B(i,j)$ is $1 + 2(i_0 - i)$ and $T(G^g(i,j), B(i,j)) \leq m + c_t(i_0 - i)$ for any $0 \leq i \leq i_0 - 1$. By Remark 4.7, we can then claim the following.

(i) The height of the box $B(i,j)$ is bounded above by $1 + 2c_r \ln(W_s(G(i,j))$;

(ii) $T(G^g(i,j), B(i,j))$ is bounded above by $m + c_t \ln(W_s(G(i,j)))$.

If a red-red edge e is created in $G^g(i,j)$ by connecting two red-blue edges (one in $G^g(i_0, 2j-1)$ and one in $G^g(i_0, 2j)$), then the turning number of the resulting edge e is the sum of the two turning numbers of the two red-blue edges in $G^g(i_0, 2j-1)$ and $G^g(i_0, 2j)$, as well as an addition of at most 6, as shown in Theorem 8.2 (i). By the inequality given in (ii) above, the turning number of the edge e is then bounded above by $2m + 2c_t(i_0 - i - 1) + 6$. However the turning number of e no longer changes in the subsequent reconnection process. We can summarize this as follows:

(iii) Let $G(i,j)$ be a BRT-graph that is subdivided into $G(i+1, 2j-1)$ and $G(i+1, 2j)$. Then for any newly created red-red edge e in the construction process of $G^g(i,j)$ we have

$$tr(e) \leq 2m + 6 + 2c_t(c_r \ln(W_s(G(i,j))) - 1).$$

In the reconstruction of $G^g(i,j)$ from $G^g(i+1, 2j-1)$ and $G^g(i+1, 2j)$, for each new red-red edge e created, we need to add up to $tr(e)$ many gridlines to place e on the lattice. The number of new red-red edges created at that stage is the same as the number of red-red edges cut by γ'. Since the number of edges cut by γ' is proportional to the square root of the total number of the vertices in the BRT-graph $G(i,j)$, by Lemma 4.2, the number of edges cut is proportional to the square root of the red vertices of $G(i,j)$. Thus the total number of gridlines which may have to be added to create the rectangle $R(i,j)$ from the rectangles $R(i+1, 2j-1)$ and $R(i+1, 2j)$ is at most

$$c \cdot (\ln(W_s(G(i,j)))\sqrt{W_s(G(i,j))} \tag{1}$$

for some constant $c > 0$ that only depends on the construction algorithm (by the inequalities we obtained from (i)–(iii) above).

Definition 8.6. Let $A(n)$ be the minimum over all positive integers p with the property that if the area of a rectangle R with aspect ratio $\sigma_R \geq 1/6$ is equal to or greater than p, then any BRT-graph G with n red vertices whose degrees are at most 12 has a grid like embedding in a box $B = R \times [0, c_h]$ where c_h is a positive integer and $c_h \leq 2\lceil \frac{\ln(n)}{\ln(6/5)} \rceil + 1$.

In the following theorems α or α_i is always a number in [1/6, 5/6]. However only those values in [1/6, 5/6] whose product with n is an integer make sense where n is the number of red vertices of the graph that is subdivided. The reader should keep this in mind in the statement and proof of Theorem 8.7 below.

Theorem 8.7. *There exists a constant integer N_0 such that the function $A'(n)$ defined by*

$$A'(n) = \begin{cases} N_0 & \text{if } n \leq W_0, \\ \max_{1/6 \leq \alpha \leq 5/6} (\sqrt{A'(\alpha n) + A'((1-\alpha)n)} + c\sqrt{6n}\ln(n))^2 & \text{if } n > W_0 \end{cases}$$

bounds $A(n)$ above, where c is the same constant used in Equation 1.

Proof. We will prove this theorem inductively. We choose N_0 as the constant guaranteed by Lemma 8.5. By definition, we have $A(k) \leq A'(k) = N_0$ if $k \leq W_0$. Now assume that $A(k) \leq A'(k)$ is true for any $k \leq n-1$ for $n \geq W_0 + 1$, we need to prove that $A(n) \leq A'(n)$.

Let $\sigma \leq 1/6$ be any given aspect ratio and R a rectangle with area $A'(n)$ and an aspect ratio σ. Let G be a BRT-graph with n red vertices. We know that there exists a subdivision of G that divides G into two BRT-graphs G_1 and G_2 with αn and $(1-\alpha)n$ red vertices respectively for some $\alpha \in [1/6, 5/6]$. Let R_0 be a rectangle with aspect ratio σ and area $A'(\alpha n) + A'((1-\alpha)n)$. By Lemma 8.4, R_0 can be divided into two rectangles R_1 and R_2 whose aspect ratios are in $[1/6, 1]$ and whose areas are $A'(\alpha n)$ and $A'((1-\alpha)n)$ respectively. Thus by our induction hypothesis, there exist grid-like embeddings G_1^g, G_2^g of G_1, G_2 respectively in the rectangular boxes B_1, B_2 whose bases are R_1, R_2 and whose heights are at most $2\lceil \frac{\ln(\alpha n)}{\ln(6/5)} \rceil + 1$, $2\lceil \frac{\ln((1-\alpha)n)}{\ln(6/5)} \rceil + 1$ respectively. Suppose that R_0 is placed in such a way that its longer side is parallel to the x-axis as shown in Figure 27. We will now extend R_0 to a new rectangle R' by adding a strip of width $c\sqrt{n}\ln(n)$ to its top and adding a strip of width $(c/\sigma)\sqrt{n}\ln(n)$ to its right. The strip added to the right of R_0 is thicker than the strip added to its top since $c/\sigma > c$. Observe that R' also has aspect ratio σ.

We know that we can obtain a grid-like embedding of G from G_1^g (which is bounded in B_1 with R_1 as its base) and G_2^g (which is bounded in B_2 with R_2 as its base). At most $c\sqrt{n}\ln(n)$ new horizontal and $c\sqrt{n}\ln(n)$ new vertical grid lines are needed to accommodate the red-red edges (which need to be put on the lattice).

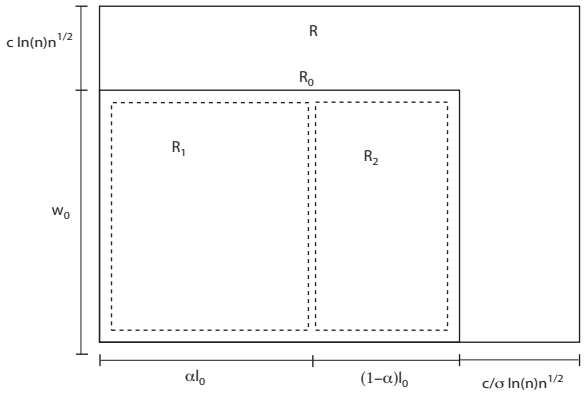

FIGURE 27. The rectangles R_0, R_1, R_2 and R'. The rectangles R_1 and R_2 are the base rectangles of the boxes B_1 and B_2.

This means that the base of the new rectangular box B (that houses this new grid-like embedding of G) can be fit into R'. Furthermore, the height of B is 2 plus the larger of the heights of B_1 and B_2. Say the height of B_1 is larger. Then the height of B is at most $2\lceil\frac{\ln(\alpha n)}{\ln(6/5)}\rceil+3$. Since $\alpha \le 5/6$, $\ln(\alpha n) \le \ln n + \ln(5/6) = \ln n - \ln(6/5)$. Thus the height of B is at most $2\lceil\frac{\ln(\alpha n)}{\ln(6/5)}\rceil+3 \le 2\lceil\frac{\ln(n)}{\ln(6/5)}-1\rceil+3 = 2\lceil\frac{\ln(n)}{\ln(6/5)}\rceil+1$. In other words, G has a grid-like embedding in the box B' with R' as its base and with a height at most $2\lceil\frac{\ln(n)}{\ln(6/5)}\rceil+1$. Let w_0 and ℓ_0 be the width and length of R_0 respectively. Then $\ell_0 = w_0/\sigma$ and $A'(\alpha n) + A'((1-\alpha)n) = \ell_0 w_0 = w_0^2/\sigma$, so $w_0 = \sqrt{\sigma(A'(\alpha n) + A'((1-\alpha)n))}$. Thus the area of R' is

$$\begin{aligned} & (w_0/\sigma + (c/\sigma)\sqrt{n}\ln(n))(w_0 + c\sqrt{n}\ln(n)) \\ = \;& (w_0 + c\sqrt{n}\ln(n))^2/\sigma \\ = \;& (\sqrt{\sigma(A'(\alpha n) + A'((1-\alpha)n))} + c\sqrt{n}\ln(n))^2/\sigma \\ = \;& (\sqrt{A'(\alpha n) + A'((1-\alpha)n)} + c\sqrt{n/\sigma}\ln(n))^2. \end{aligned}$$

However since $1/6 \le \sigma$, $n/\sigma \le 6n$, the area of R' is bounded above by

$$\begin{aligned} & (\sqrt{A'(\alpha n) + A'((1-\alpha)n)} + c\sqrt{6n}\ln(n))^2 \\ \le \;& \max_{1/6\le\alpha\le 5/6} (\sqrt{A'(\alpha n) + A'((1-\alpha)n)} + c\sqrt{6n}\ln(n))^2 = A'(n). \end{aligned}$$

Since R and R' have the same aspect ratio and R has a larger area, R' can be fit into R. Therefore, G has a grid-like embedding in a box with base R and height at most $2\lceil\frac{\ln(n)}{\ln(6/5)}\rceil+1$. This proves that $A(n) \le A'(n)$. □

The next theorem gives the function $A'(n)$ (hence $A(n)$) an explicit bound.

Theorem 8.8. *There exists a constant $d > 0$ such that $A'(n) \le dn(\ln(n))^4$. It follows that $A(n) \le dn(\ln(n))^4$ as well.*

PROOF. Following the proof given in [**17**] we define a function $B(n)$ as follows: For $n \leq W_0$, $B(n) = \sqrt{N_0}$ and for $n > W_0$

$$B(n) = \max_{1/6 \leq \alpha \leq 5/6} (B(\alpha n) + c\sqrt{6}\ln(n)). \tag{2}$$

We show that $A'(n) \leq n(B(n))^2$ for all $n \geq W_0$ by induction. Clearly this is true for $n = W_0$. Assume that $A'(k) \leq n(B(k))^2$ is true for all values of k such that $W_0 \leq k < n$. For $k = n$ we have:

$$\begin{aligned} A'(n) &= \max_{1/6 \leq \alpha \leq 5/6} (\sqrt{A'(\alpha n) + A'((1-\alpha)n)} + c\sqrt{6n}\ln(n))^2 \\ &\leq \max_{1/6 \leq \alpha \leq 5/6} (\sqrt{\alpha n(B(\alpha n))^2 + (1-\alpha)n(B((1-\alpha)n))^2} + c\sqrt{6n}\ln(n))^2 \\ &\leq \max_{1/6 \leq \alpha \leq 5/6} (\sqrt{n(B(\alpha n))^2} + c\sqrt{6n}\ln(n))^2 \\ &\leq \max_{1/6 \leq \alpha \leq 5/6} n(B(\alpha n) + c\sqrt{6}\ln(n))^2 = n(B(n))^2. \end{aligned}$$

The third line in the above inequalities can be explained as follows: If $B(\alpha n) \geq B((1-\alpha)n)$ for the value of α realizing the maximum then this is obvious. If $B(\alpha n) < B((1-\alpha)n)$ then the same result follows where α is replaced by $(1-\alpha)$. Then a change of variable of $(1-\alpha)$ for α produces the same result.

Now $B(n)$ needs to be estimated. Using Equation (2) repeatedly for different values of α results in:

$$B(n) = \sqrt{6}c(\ln(n) + \ln(\alpha_1 n) + \ln(\alpha_1\alpha_2 n) + \ldots + \ln(\alpha_1 \ldots \alpha_s n) + N_0,$$

where s is the depth of the recursion and each value α_i is the value of α that realizes the maximum at each stage of the recursion. Since all $\alpha_i \leq 1$ we have for some constant c'

$$B(n) \leq \sqrt{6}c \cdot s(\ln(n)) + N_0 \leq c'(\ln(n))^2.$$

From this it follows that there exists a constant $d > 0$ such that $A'(n) \leq n(B(n))^2 \leq d \cdot n(\ln(n))^4$. □

Corollary 8.9. Let G be a 4-regular plane graph with n vertices. Then there exists a realization of G on the cubic lattice $\mathbb{Z}^3$ which is contained in a rectangular box whose volume is bounded above by $O(n\ln^5 n)$.

PROOF. First, we change G to a BRT-graph G' by triangulation. Next we construct a grid-like embedding of G' in the lattice in a box $B = R \times I$ by the previously described algorithm. The number of vertices in G is equal to the number of red vertices in G'. The algorithm described in the paper generates a rectangular box with a height of at most $c_h \ln n$ for some constant $c_h > 0$. From Theorem 8.7 we know that the area of the rectangle R is of the order $O(n\ln^4 n)$ and thus the volume of the box containing the grid-like embedding of G is bounded above by $O(n\ln^5 n)$.

The lattice embedding described in the prior section assumes that edge segments in the red rectangles are not on lattice. In order to obtain a complete lattice

embedding of G, the edges which are added to G in the triangulation to obtain the BRT-graph G' are removed from the embedding. Now each red rectangle only intersects 4 edges and these edges can be re-arranged in the rectangle such that they connect to the red vertex using only lattice connections. Thus the lattice embedding of G fits into the same rectangular box as the grid-like embedding of G. □

Let D be a knot diagram of $\mathcal{K}$ with n crossings. D can be thought of as a 4-regular plane graph and by Corollary 8.9 there exists a lattice embedding of the 4-regular plane graph D in a rectangular box with a volume of order $O(n \ln^5 n)$. In order to change this lattice embedding of the graph D to the embedding of the knot $\mathcal{K}$, we need to recover the crossings of the original knot diagram from the vertices of the embedded graph. In order to accomplish this, the edges at a vertex v are locally modified as shown in Figure 28. One unit away from the vertex v the edge is rerouted through the plane $z = 0.5$ to recover the desired crossing. The space between $z = 0$ and $z = 0.5$ and the space between $z = 0.5$ and $z = 1$ are then stretched to one unit thick each (so that $z = 0.5$ becomes the lattice plane $z = 1$ afterwards). The new rectangular box containing the recovered knot is identical to the previous one except that its height has increased by one. The volume of the surrounding box is still bounded above by $O(n \ln^5 n)$.

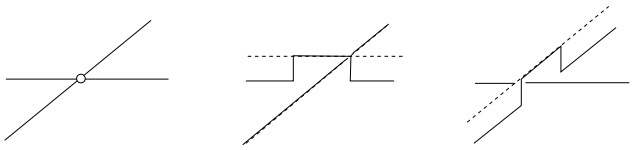

FIGURE 28. Reroute the edges at a vertex to recover the desired under/over crossing.

The length of the lattice embedding of a diagram D is bounded above by the volume of the box surrounding the lattice embedding of D. Furthermore, the rope-length of a knot $\mathcal{K}$ is bounded above by twice the length of the lattice embedding. The result of our main theorem (Theorem 8.3) then follows.

9. Some open questions

Theorem 8.3 answers the following question raised in [**9, 10**] negatively.

9.1. Question. For any $1 < p \leq 3/2$, does there exist a family of infinitely many knots (links) such that $L(K) \geq O(Cr(K))^p)$ for knots in this family?

However the following question also raised in [**9, 10**] remains open:

9.2. Question. Is it true that $\sup\{\frac{L(K)}{Cr(K)}\} = \infty$ (where the supremum is taken over all knots and links)?

Equivalently we can ask the following:

9.3. Question. Does there exist a $p > 0$ and a constant $a > 0$ such that there exists an infinite family of knots and links such that for any member K in the family, $L(K) \geq a \cdot (Cr(K)) \cdot \ln(Cr(K))^p$?

Since we know that there exist knots $\mathcal{K}$ with ropelength of order $O(Cr(\mathcal{K}))$, the only possible further improvement on Theorem 8.3 is to reduce the power on the $\ln(Cr(K))$ term. In [**14**], a numerical study suggests the possibility of a ropelength upper bound of the form $O(Cr(K)\ln^2(Cr(K)))$. We thus end this paper with the following question:

9.4. Question. Can we improve the ropelength upper bound to $L(K) \geq a \cdot (Cr(K)) \cdot \ln(Cr(K))^2$?

References

[1] J. Arsuaga, R. K. Tan, M. Vazquez, D. W. Sumners and S. Harvey, *Investigation of viral DNA packaging using molecular mechanics models*, Biophys. Chem. **101** (2002), 475–484.

[2] J. Arsuaga, M. Vazquez, S. Trigueros, D. W. Sumners and J. Roca, *Knotting probability of DNA molecules confined in restricted volumes: DNA knotting in phage capsids.* Proc. Natl. Acad. Sci. USA **99** (2002), 5373–5377.

[3] J. Arsuaga, M. Vazquez, P. McGuirk, S. Trigueros, D. W. Sumners and J. Roca, *DNA knots reveal a chiral organization of DNA in phage capsids*, Proc. Natl. Acad. Sci. USA **102** (2005), 9165–9169.

[4] G. Buck, *F*our-thirds Power Law for Knots and Links, Nature **392** (1998), 238–239.

[5] G. Buck, *Four-thirds Power Law for Knots and Links*, Nature, **392** (1998), pp. 238-239.

[6] J. Cantarella, R. B. Kusner and J. M. Sullivan, *Tight Knot Values Deviate from Linear Relations*, Nature **392** (1998), 237–238.

[7] J. Cantarella, R. B. Kusner and J. M. Sullivan, *On the Minimum Ropelength of Knots and Links*, Invent. Math. **150**(2) (2002), 257–286.

[8] Y. Diao and C. Ernst, *The Complexity of Lattice Knots*, Topology and its Applications **90**(1-3) (1998), 1–9.

[9] Y. Diao and C. Ernst, *Realizable Powers of Rope Lengths by Nontrivial Knot Families*, Journal of Geometry and Topology **4**(2) (2004), 197–208.

[10] Y. Diao and C. Ernst, *Hamiltonian cycles in Conway's algebraic knots and their implications on ropelength*, J Knot Theory and Ramifications **15**(1) (2006), 121–142.

[11] Y. Diao, C. Ernst and E. J. Janse Van Rensburg, *Thicknesses of Knots*, Math. Proc. Camb. Phil. Soc. **126** (1999), 293–310.

[12] Y. Diao, C. Ernst and M. Thistlethwaite, *The linear growth in the length of a family of thick knots*, J Knot Theory and Ramifications **12**(5) (2003), 709–715.

[13] Y. Diao, C. Ernst and X. Yu, *Hamiltonian Knot Projections and Lengths of Thick Knots*, Topology and its Applications **136** (2004), 7 – 36.

[14] Y. Diao, C. Ernst, R. Kavuluruast and U. Ziegler, *Numerical upper bounds on ropelengths of large physical knots* , J. Phys. A: Math. Gen. **39** (2006), 4829–4843.

[15] Y. Diao, C. Ernst and U. Ziegler, *The Linearity of the Ropelengths of Conway Algebraic Knots in Terms of Their Crossing Numbers*, preprint.

[16] C. Ernst and D. W. Sumners, *A calculus for rational tangles with applications to DNA,* Math. Proc. Camb. Phil. Soc. **108** (1990), pp. 489–515.

[17] C. Leiserson, *Area efficient graph layouts (for VSLI)*, Proc. IEEE Syrup. on Foundations of Computer Science (1980), 270–281.

[18] R. Litherland, J. Simon, O. Durumeric, and E. Rawdon, *Thickness of Knots*, Topology and its Applications **91**(3) (1999), 233–244.

[19] G. L. Miller, *Finding small simple cycle separators for* 2*-connected planar graphs*, J. Comput. System Sci. **32**(3) (1986), 265–279.

[20] V.V. Rybenkov, N.R. Cozzarelli and A.V. Vologodskii, *Probability of DNA knotting and the effective diameter of the DNA double helix,* Proc. Natl. Acad. Sci. USA **90** (1993), pp. 5307–5311.

[21] D. W. Sumners, C. Ernst, S. J. Spengler and N. R. Cozzarelli, *Analysis of the mechanism of DNA recombination using tangles,* Quart. Rev. Biophysics **28**, 3 (1995), pp. 253–313.

Department of Mathematics, University of North Carolina at Charlotte, Charlotte, NC28223

E-mail address: ydiao@uncc.edu

Department of Mathematics and Computer Science, Western Kentucky University, Bowling Green, KY 42101

E-mail address: claus.ernst@wku.edu

Department of Mathematics and Computer Science, Western Kentucky University, Bowling Green, KY 42101

E-mail address: Attila.por@wku.edu

Department of Mathematics and Computer Science, Western Kentucky University, Bowling Green, KY 42101

E-mail address: Uta.Ziegler@wku.edu